Applied Clay Science 229 (2022) 106686

Contents lists available at ScienceDirect

Applied Clay Science

journal homepage: www.elsevier.com/locate/clay

Review article

Adsorption of organic water pollutants by clays and clay minerals composites: A comprehensive review

Dina Ewis, Muneer M. Ba-Abbad, Abdelbaki Benamor, Muftah H. El-Naas *

Gas Processing Center, College of Engineering, Qatar University, P.O.Box 2713, Doha, Qatar

ARTICLE INFO

Keywords:
Adsorption
Clay composites
Organic pollutants
Water pollutants
Adsorbents cost.

ABSTRACT

Clays and clay minerals are inexpensive, non-toxic, and naturally occurring minerals that have been utilized in water remediation as adsorbents. However, clays and clay minerals and those modified with heat, surfactants, acids, or organic-inorganic modifiers exhibit low adsorption capacity and re-generation ability towards organic water pollutants. The development of clays and clay minerals composites has gained considerable attention in recent years due to their enhanced adsorption capacity, ease of recovery from aqueous solution and improved physiochemical properties relative to raw and modified clays and clay minerals. This review aims to assess recent literature on clays and clay minerals composites including bentonite, montmorillonite and kaolinite intercalated with carbonaceous, metals, metal oxides, chitosan and polymeric materials and appraise their adsorption performance towards organic water pollutants. The review examines the effect of the composites' physicochemical properties on the adsorption performance and evaluates the adsorption mechanism as well as regeneration methods. The review also attempts to highlight the current progress in this area by assessing the outcomes of recently published articles and outline the research gaps for future research.

1. Introduction

The rapid development of industry and population growth have increased the demand for clean water resources for domestic and agriculture use (Jun et al., 2020). The situation is becoming worse as industrial sectors continue to discharge toxic, hazardous, and persistent water pollutants into water bodies, which elevated water scarcity to become a greater challenge that nearly all countries encounter to a certain degree (Askalany et al., 2020; Khodabakhshloo et al., 2021; Wang et al., 2021). The United Nations (2006) predicted that by 2025, two-thirds of the world's population would suffer from water shortages with the continuous increase in water pollution levels (Bullock, 2006). Water pollutants, including organic and inorganic contaminants, are generated mainly from industrial effluents and human activities, such as the excessive use of pesticides and fertilizers (Venancio et al., 2013). In particular, large quantities of industrial effluents containing organic pollutants including pesticides, antibiotics, hydrocarbon, herbicides, dyes, phenols, proteins, and detergents are discharged into water bodies, which might consume the available dissolved oxygen to degrade. This causes the depletion of dissolved oxygen level available for aquatic life and subsequently threat the marine environment (Lin et al., 2014; Rahmani et al., 2020a). In order to maintain clean water resources and limit the discharge of highly contaminated wastewater into water bodies, recent research work focuses on treating the huge amount of industrial wastewater generated from various industries through cost-effective and environmentally friendly processes prior to discharge. In this context, several treatment technologies have been adopted to remedy wastewater including membrane, floatation-coagulation, electrocoagulation and biological treatment (Combatt et al., 2020; Ozbey-Unal et al., 2020; Saleh et al., 2020; Wang et al., 2020b; Ewis et al., 2021). Despite the high treatment efficiency of these technologies, they are often associated with several concerns, such as high-energy consumption, high capital cost, and scale-up challenges. Adsorption technology has attracted a great deal of interest due to its simplicity, cost and energy efficiency, environmentally friendly nature and high treatment efficiency (Yu et al., 2021). In the industry, wastewater process involves three stages: pre-treatment, main treatment, and final polishing. Adsorption is used in the polishing step to eliminate the ultra-small particles. Among the available adsorbents, clays and clay minerals are inexpensive, non-toxic and naturally occurring minerals that have been utilized in water remediation applications (Lazaratou et al., 2020).

Extensive work has been done in investigating the adsorptive

* Corresponding author.
E-mail address: muftah@qu.edu.qa (M.H. El-Naas).

https://doi.org/10.1016/j.clay.2022.106686
Received 27 February 2022; Received in revised form 14 August 2022; Accepted 16 August 2022
Available online 24 August 2022

performance of clays and clay minerals composites towards organic and inorganic water pollutants. Clays including bentonite and kaolin are hydrous aluminosilicate minerals that composed of mixtures of clay minerals, and crystals of other minerals such as quartz and metals oxides (Arif et al., 2021). While, clay minerals including montmorillonite and kaolinite are a large group of phyllosilicates family that includes planar hydrous and non-planar hydrous phyllosilicates (Chen et al., 2016). The distinct two-dimensional (2D) layer structure and unique physiochemical properties of clays and clay minerals including swelling and ion exchange capacity enable them to adsorb various organic and inorganic water pollutants (Chen et al., 2016; Ewis and Hameed, 2021). The interlayer spaces in some types of clays and clay minerals structures such as bentonite enable them to trap containments, which is known as swelling capacity (Li et al., 2018; Dietel et al., 2019). There are many factors influencing the performance of clays and clay minerals during the adsorption process including surface charge, specific surface area and swelling characteristics. In addition, they attain cation exchange capacity (CEC), which is defined as the quantity is positive ions that can be exchanged per unit mass of dry clay mineral (Cheng and Heidari, 2018). These cationic counter ions are exchanged by other cations, thus increasing the affinity of clay minerals to remove cationic organic and inorganic pollutants, such as dyes and lead, respectively (Hizal and Apak, 2006; Sakin Omer et al., 2018). Conversely, clays and clay minerals exhibit low to medium Anion Exchange Capacity (AEC) (Schell and Jordan, 1959; Rihayat et al., 2018). Hence, physical and chemical modification methods have been adopted to improve their structure and surface properties to increase their affinity towards organic water pollutants (Otunola and Ololade, 2020). However, these processes are usually associated with the use of high temperatures (120-700 °C) and chemicals (e.g. strong acids), which increase the adsorption process cost and energy requirements. In addition, thermally and chemically modified clays and clay minerals performance in real wastewater is poor due to the coexistence of multiple pollutants. Also, clay minerals tend to stay in suspension in aqueous media due to their micro size, which limits their regeneration ability and performance in fixed-bed or columns (Unuabonah and Taubert, 2014; Najafi et al., 2021). These drawbacks limited their application in the industry (Yao et al., 2014). Recently, clays and clay minerals composites have attracted a great deal of interest due to their superior properties, structure and adsorption capacity compared to those of their individual components (Kong et al., 2018; Wei et al., 2019). In addition, they possess enhanced mechanical strength, extraordinary CEC and higher stability.

Extensive research was carried out in the last decade to develop clays and clay minerals (clay/minerals) composites with the aim to remove organic water pollutants. To the best of the authors' knowledge, there are no reviews in the open literature devoted to the adsorption of organic water pollutants using clays and clay minerals composites. Most of the review papers focus on the performance of raw and modified clay/minerals for the removal of heavy metals (Uddin, 2017; Yadav et al., 2019; Otunola and Ololade, 2020), nitrate (Lazaratou et al., 2020) and synthetic dyes (Ngulube et al., 2017). In addition, only a few review papers summarized the adsorptive performance of raw and modified clay/minerals towards organic contaminants removal (Awad et al., 2019; Shen and Gao, 2019). Therefore, the main objective of this paper is to review recent research progress made on clay/minerals composites for organic water pollutants removal. This review focuses on the adsorptive performance of bentonite, montmorillonite (MT), and kaolinite intercalated with carbonaceous, metals, metal oxides, chitosan and polymeric materials. In addition, the effect of several adsorption parameters such as pH, presence of organic matter, and ionic strength on the adsorption capability of clay/minerals composites are discussed. The review also explores the clay minerals composites physiochemical properties and structural characteristics compared to the composite individual components. Furthermore, it examines the adsorption mechanism as well as the regeneration methods for clay/minerals composites. Overall, this review attempts to identify research gaps and clarify the future challenges involved in the regeneration as well as the utilization of clay/minerals composites in this area.

2. Preparation of clays and clay minerals composites

Research has focused on developing selective, and efficient clay/minerals adsorbents prepared under mild conditions. In this context, great advances have been made in modification and hybridization, ranging from surface modification to the fabrication of composites. In this section, the pretreatment of clay/minerals including purification, and surface modification has been discussed. In addition, the synthesis methods of clay minerals composites and the associated conditions are highlighted.

2.1. Pre-treatment

In most cases, analytical-grade clay/minerals are used without purification. However, prior to composite fabrication, the clay/minerals is immersed in distilled water for several hours under continuous stirring or subjected to ultrasonic waves for several hours. This is to obtain a homogenous suspension and achieve the maximum swelling capacity (Lou et al., 2015a; Ain et al., 2020a; Cao et al., 2020). For example, Rahmani et al. (2020b) carried out a purification process for montmorillonite prior to composite fabrication. The purification process included immersion of 100 g of montmorillonite in 1 l of distilled water under vigorous stirring for 1 h at room temperature. After that, the suspension was centrifuged at 5000 rpm for 15 min. Finally, the resulted slurry was dried at 80 °C for 12 h and grinded and sieved to the size of 200 meshes. This process resulted in increasing the CEC value to 85 meq/100 clay for purified clay compared to 55 meq/100 clay for unpurified clay.

Other studies used various modification techniques including acid treatment, and ion exchange to optimize the composite adsorption capacity prior to composite fabrication. Modification of clay/minerals with these methods facilitates composites fabrication, such as clay mineral-polymer composite (Ferreira et al., 2017; Hojiyev et al., 2017). In acid activation, hydrochloric acid (HCl) with a typical concentration of 1 M is used in the pre-treatment step to remove the minerals impurities. Then, the mixture is exposed to ultrasonic waves for several minutes to reduce the agglomeration of clay minerals particles, which increases the specific surface area. Khatamian et al. (2019) reported that in presence of sonication, the specific surface area increased for raw bentonite and iron oxide/bentonite composite by around 18% and 40%, respectively. Besides, as mentioned above, clay minerals attain CEC, which allows exchanging the inorganic cations present in the interlayer space with various materials including metals, surfactants, dyes, and humic acid to produce intercalated clays. The enhancement in adsorption capacity of the intercalated clays is mainly due to the improvement of surface hydrophobicity, and the addition of new functional groups that add new possible interaction. For instance, Ain et al. (2020a) claimed that the hydrophobicity of 3-acrlyamidopropyl trimethyl ammonium chloride (APTMA) intercalated bentonite increased, which reduced the sedimentation rate of intercalated bentonite allowing better contact between the adsorbate and the adsorbent. In addition, the study showed that despite the dramatic reduction in pore volume and specific surface area of the intercalated bentonite, the average pore diameter and pore width increased. The SEM images indicated that intercalated bentonite attained exfoliated, flaky, and less packed morphology, unlike raw bentonite that has a smooth and compact structure. (Wan et al., 2015) reported that pillaring bentonite with Al through cation exchange process enhanced rhodamine B molecules adsorption. The study highlighted that Al pillared bentonite had a coarse porous surface unlike raw bentonite, which is essential for organic pollutants adsorption. For clay mineral composites synthesis, most of the studies used either acid activation or ion exchange prior to composite fabrication.

2.2. Synthesis methods

clay/minerals-metal and metal oxides composites can be synthesized via various methods including co-precipitation, co-precipitation ultrasound-assisted, liquid-phase reduction, spray drying (to synthesize spherical composites) and hydrothermal. Raw, modified, or functionalized clays can be used prior to composite synthesis. In the co-precipitation method, the clay/minerals is mixed with other precursors for several hours followed by the addition of a reducing agent. The reducing agent is either ammonia or sodium hydroxide that brings the solution pH to 11–12. However, unlike sodium hydroxide, ammonia is a better stabilizer and helps in the growth of nanoparticles (Peternele et al., 2014). Ouachtak et al. (2020) prepared magnetic montmorillonite (γ-Fe_2O_3@Mt) composite through conventional co-precipitation. The process involved dispersing montmorillonite in deionized water. Then, 1 M of $FeCl_2.4H_2O$ and 2 M of $FeCl_3$ at a ratio of 1:2 was dissolved in 100 ml deionized water and added to the montmorillonite suspension. Finally, 2 M of ammonia was added under stirring at 60 °C for 4 h allowing the reaction to occur. In another study, similar steps was followed for magnetic bentonite fabrication, but the reaction occurred in ultrasonic bath for 3 h (Khatamian et al., 2019). The study revealed that the use of ultrasonic waves increased the composite specific surface area, allowed uniform and homogenous distribution of iron oxide nanoparticles over bentonite surface, and resulted in homogenous and smooth distribution of iron oxide nanoparticles on bentonite inner wall without blocking their cavities. Hydrothermal method is related to mixing all precursors for several hours followed by transferring the mixture to an autoclave (Liu et al., 2021; Li et al., 2022). Then, the autoclave is transferred to an oven at a high temperature (e.g. 250 °C) for several hours (Fei et al., 2020). In the liquid-phase method, the precursors are mixed in miscible liquid for several minutes (e.g.15 min) followed by the addition of a reducing agent (e.g. sodium borohydride) dropwise under a nitrogen environment (Chen et al., 2013). Moreover, clay composites can be synthesized in spherical form. A study conducted by Wang et al. (2019) reported the synthesis of spherical montmorillonite-supported nanosilver through spray-drying technology. The core principle of this technology is rapidly heating the slurry via direct injection of small droplets. Initially, the slurry was prepared by sonicating montmorillonite mixed with 98 mL ethanol and 2 mL of sulfuric acid for 60 min. Then, the slurry was fed into a spray-dryer using 105 °C drying temperature. It was found that spherical montmorillonite attained higher specific surface area and pore volume compared to raw montmorillonite even after silver nanoparticles loading.

The fabrication of clay/minerals-chitosan and clay/minerals-polymeric composites are mainly through three techniques: cross-linking, adsorption, and in-situ polymerization. Cross-linking is related to using cross-linking compounds, such as glutaraldehyde, that covalently bonds clay with the polymer chain (Liu et al., 2015b). Usually, the mixture should be left for 24 h at a relatively high temperature (≈60 °C) for cross-linking reaction to occur. In the adsorption technique, the polymer solution is mixed with dispersed clay in which physical attraction including attraction electrostatic and Van der Waals interaction is formed (Zhang et al., 2016a). While the in-situ polymerization method, the polymer is mixed with the clay mineral suspension followed by the addition of a polymerization initiator, such as ammonium persulphate to boost polymerization reaction (Vanamudan et al., 2014). In all the above-mentioned methods, some studies used sodium hydroxide to neutralize the solution pH in order to enhance the rate of polymerization (Khanlari and Dubé, 2015). For instance, clay/minerals-chitosan composites are commonly prepared as follows: chitosan was dissolved in (1–2%) (*v*/v) acetic acid solution under magnetic agitation for several hours. Bentonite or montmorillonite was added to 50–100 ml of deionized water at 60 °C for a few minutes followed by adjusting the solution pH to 5.0 using NaOH, which boosts precipitation reaction. Then, chitosan mixture was added to clay mineral suspension under mechanical stirring (≈1200 rpm) at 60 °C for several hours (e.g. 4 h). Finally, the mixture was dried in an oven at 60 °C and left overnight (Dotto et al., 2016; Dehghani et al., 2018; El-Kousy et al., 2020).

clay/minerals-carbonaceous composites are commonly synthesized through wet impregnation method. Typically, the process begins with dispersing the carbonaceous source and the clay mineral in deionized water using an ultrasonic bath in separate beakers. The clay suspension is sonicated for around 8 h. Then, the carbonaceous suspension is added dropwise to the clay suspension under continuous stirring. Finally, the slurry is dried overnight at approximately 80 °C in an oven (Ashiq et al., 2019; Neelaveni et al., 2019; Xu et al., 2019).

3. Adsorption performance of clays and clay minerals composites

Clays and clay minerals composites have received attention due to their superior adsorptive performance and physiochemical characteristics compared to those of their individual components. Recently, considerable efforts have been dedicated to fabricating clay/minerals composites by combining clay minerals with two or more materials. Metals, metals oxides, chitosan, polymeric and carbonaceous materials are the most common materials combined with clay minerals for adsorption of organic water pollutants. Among the available clay minerals, bentonite, montmorillonite, and kaolinite are the most common adsorbents that are used in wastewater remediation due to their availability and good adsorption characteristics (Ngulube et al., 2017). In this section, the physiochemical characteristics of clay minerals composites and their adsorptive performance towards organic water pollutants are critically analyzed and summarized.

3.1. Clay/minerals-metals and metal oxide composites

Metals and Metals oxides have a broad range of applications including gas sensors, catalysis and environmental remediation (Zhang et al., 2016c; Daraee et al., 2019; Zhang et al., 2020a; Almahri, 2022). They have been utilized extensively in environmental remediation as adsorbents due to their remarkable characteristics including high specific surface area, good mechanical and chemical stability, non-toxicity nature, and unique surface characteristics (Oyewo et al., 2020). Usually, non-magnetic spent adsorbents are separated from aqueous solution through centrifugation and filtration methods, which are time consuming and expensive (Duman et al., 2016a, 2016b, 2019). Alternatively, magnetic metals oxides, such as iron oxide nanoparticles, are widely used in wastewater treatment as adsorbents due to their magnetic property that facilities their separation from aqueous solution by an external magnetic field. Over the past decade, clay/minerals-metals oxides as composite material have shown significant potential as a highly selective adsorbent for the effective removal of organic pollutants. Bentonite, montmorillonite, and kaolinite are the common types of clay minerals that have been combined with metals oxides for efficient removal of organic contaminants.

3.1.1. Bentonite/metals and metal oxide composites

To date, the adsorption behavior of various types of organic pollutants on bentonite/metals oxides composites has been studied extensively. Most of the studies focus on the fabrication of Fe_3O_4/Bentonite composite to facilitate the composite separation from aqueous solution due to magnetic property of Fe_3O_4 nanoparticles, meanwhile, achieving high removal of an organic contaminant. The studies related to the fabrication Fe_3O_4/bentonite composites reported that the composite exhibits super-magnetic behavior, which suggests that the composite could be manipulated by an external magnetic field (Wan et al., 2015; Khatamian et al., 2019; Ain et al., 2020a; Ewis et al., 2020). Furthermore, Fe_3O_4/bentonite composites attained a magnetization saturation value lower than Fe_3O_4 nanoparticles, which is due to the existence of nonmagnetic bentonite.

The adsorbent specific surface area is one of the important factors

that influence the adsorption capacity as it determines the number of effective collisions between the active sites and contaminants (Muhammad et al., 2019). For instance, Wan et al. (2015) attributed the increase rhodamine B adsorption from 4.28 mg/g to 62.15 mg/g using Fe_3O_4 nanoparticle and Fe_3O_4/bentonite, respectively, to the increase in the composite specific surface area compared to Fe_3O_4 nanoparticle. However, other studies reported that Fe_3O_4/bentonite composite attained adsorption capacity greater than the composite individual components, even though, the composite specific surface area is less than Fe_3O_4 nanoparticles and bentonite (Ain et al., 2020a; Cao et al., 2020). The authors attributed the enhancement in the composite adsorption capacity to the increase in the composite pore volume and active sites available for adsorption. The decrease in the composite specific surface area could be as a result of intercalating Fe_3O_4 nanoparticles within bentonite interlayer spacing, which decreases specific surface area. It is worth mentioning that the pillaring agents have a great impact on the surface structure and physical properties of bentonite. It was reported that the closely packed structure of bentonite was loosened and various size pores were formed as a result of pillaring by Ti-pillars (Tomul et al., 2016). Also, after the addition of Cu, Ag, and Fe, the structure conserved its pore structure without obvious changes. However, there were significant changes in the specific surface area and external surface area. The study revealed that the external surface area increases with impregnation, especially for silver impregnation and iron ion exchange procedure, which might be due to the distribution of these elements within the layers forming mesopores. The study emphasized that the composite structure and physical properties change depending on the nature and the distribution of the pillaring agents, which influence their adsorptive performance. Furthermore, in bentonite/metals and metal oxides based composites, bentonite acts as a support for metals oxides due to bentonite large specific surface area as revealed by Scanning Electron Microscope (SEM) images. In addition, metal oxides nanoparticles could agglomerate during their deposition on bentonite surface due to either their high surface energy or the high magnetic force they attain, which affects the adsorption process efficiency. The agglomeration of metals oxides nanoparticles could be reduced using ultrasound waves during the synthesis which allows a uniform distribution of metals oxides nanoparticles over bentonite surface (Ain et al., 2020b). However, uniform distribution of metals nanoparticles on bentonite clay could be obtained by using reducing agents during the synthesis without the application of ultrasound, which enhances the adsorption performance. For instance, Gopal et al. (2020) reported that iron (Fe) and Lead (Pd) attained a spherical shape with less aggregation over bentonite clay. Furthermore, the deposition of Fe and Pd metals over bentonite clay increased the specific surface area and enhanced the tetracycline removal from aqueous solution; after the deposition of Fe/Pd metals on bentonite clay, the composite attained a removal percentage of tetracycline 3 times larger than the removal percentage of Fe/Pd.

The surface functional group and hydrophobicity were greatly enhanced after loading bentonite with metal oxide, which resulted in enhanced adsorption capacity. Ain et al. (2020a) reported that the increase in crystal violet adsorption is due to the abundant active functional groups provided by the composite compared to raw bentonite. Furthermore, the study highlighted that the swelling behavior of bentonite was affected significantly after the addition of Fe_3O_4 NPs. The study showed that the magnetization and modification of bentonite through silylation caused the composite to have high water dispersion and static volume. Unlike raw bentonite that tends to settle down after reaching the saturation point and maximum swelling capacity, Fe_3O_4/bentonite did not show any sedimentation and remained suspended, which led to better adsorption performance.

The co-existing of multiple pollutants can reduce the adsorption performance of raw bentonite significantly; however, that reduction could be minimized for bentonite/metal oxides compared to raw bentonite. As observed in one of the studies, in a tetra-component system, the adsorption capacity was reduced for more than half of the single-component system for raw bentonite, but the composite (Fe_3O_4/bentonite) experienced lower reduction and proved resilient (Ain et al., 2020a). Also, increasing the ionic strength of the suspension can enhance the adsorption of dyes on bentonite/ metal oxides surface. In the same study, it was reported that the existence of heavy metals enhanced the composite adsorption capacity towards dyes due to the formation of dye dimer molecules, which was not the case for raw bentonite.

The water matrixes can significantly affect the metal oxides/bentonite removal capability. The removal rate of organic compounds by clay minerals composites differs significantly in different water matrices such as lake water, ground water, tap water and deionized water. This is because a large number of colloids are present in lake water, ground water and tap water, which may interfere with the bentonite/ metal oxide composite to reduce its removal capability (Gopal et al., 2020).

The solution pH has a great impact on the form of organic pollutant and the charges available on the pollutant and on the bentonite/metal oxide composite. Generally, for all bentonite/metal oxide composites reported in this review, the optimum removal capability was observed in pH between 5 and 8. For instance, the removal of crystal violet decreased as the pH increased from 2 to 6, reaching a plateau at pH 7 and then decreased with further pH increase (Ain et al., 2020b). This is because at pH lower than 7, the H^+ ions compete with cationic crystal violet resulting in a low removal percentage. Whereas at pH higher than 7, deprotonation of crystal violet and bentonite/metal oxide composite generates negative charges, which results in an electrostatic repulsion, hence reducing the removal percentage. It is worth noting that the point of zero charge (pHpzc) can help in understanding the removal percentage at different pH values. Generally, pHpzc is the pH at which the net surface charge on the surface is zero (Ain et al., 2020a). pHpzc can be determined through measuring the zeta potential of the composite, which indicates the composite potential as function of solution pH (Duman and Tunç, 2009). It is well known that the maximum adsorption of cationic dye is at pH > pHpzc due to the existence of functional groups such as hydroxyl, whereas anionic dye adsorption is maximum at pH < pHpzc due to the positivity of charged surface.

Thus, metals oxides/bentonite composites showed a high adsorption capacity towards organic water pollutants including antibiotics, phenols, and dyes. Several studies have confirmed the increase in adsorption capacity compared to the composite individual components (Wan et al., 2015; Ain et al., 2020a; Ewis et al., 2020; Gopal et al., 2020). For instance, Ewis et al. (2020) reported that Fe_3O_4/bentonite attained around 71% removal of diesel oil, compared to 28% removal using Fe_3O_4 nanoparticles due to the addition of bentonite clay. Furthermore, the increase in the specific surface area does not necessary indicate that the composite adsorptive performance is enhanced compared to its individual components. In fact, several factors are important including the pore volume, pore diameter and surface functional groups.

It is worth mentioning that after adsorption new surface functional groups might appear and/or the existing functional groups intensity might increase. These changes can be detected through FTIR spectra and can be used to reveal the adsorption mechanism. Table 1 summarizes the adsorption performance of bentonite/metals and metal oxides composites towards organic water pollutants.

3.1.2. Montmorillonite/metals and metal oxide composites

Similar to bentonite, montmorillonite acts as a support for metals and metals oxides due to its large specific surface area. Several studies investigated the performance of montmorillonite integrated with iron oxides nanoparticles (Fe_3O_4/Montmorillonite) that possess magnetic behavior, which facilitates its separation from aqueous solution. Unlike Fe_3O_4/bentonite composite, a uniform distribution of Iron oxide nanoparticles (Fe_3O_4 NPs) over montmorillonite was obtained in a conventional co-precipitation synthesis process without the application of

Table 1
Adsorption performance of bentonite/metals and metal oxides composites towards organic water pollutants.

Composite	Pollutant	Type of water	Specific surface area (m^2/g)	Magnetic saturation (emu/g)	Experiment conditions					Adsorption capacity q_{max} (mg/g)	Mechanism	Surface functional group	Ref.
					Dosage (g)	pH	Initial concentration (mg/L)	Time (min)	Temperature (°C)				
Fe_3O_4/bentonite	Rhodamine B	Synthetic	53.02	30.9	0.2	9–10	5–400	120	25	62.2	–	–	(Wan et al., 2015)
Fe_3O_4/bentonite	Methylene Blue	Synthetic	100.6	28	3	7	20	20	–	38	Hydrogen bond	OH	(Lou et al., 2015b)
Ti-pillared bentonite (PTi-PILC.) by hydrolysis of titanium (IV) propoxide (PTi)			201							8.1			
Ti-pillared bentonite (ETi-PILC) by hydrolysis of titanium (IV) ethoxide (ETi)			138							7.9			
Cu modified Ti-pillared bentonite (PCu/Ti-PILC)	Bisphenol A	Synthetic	179	–	5 g/L	4	5–50	120	25	8.3	–	–	(Tomul et al., 2016)
Cu Incorporation to Ti-pillared bentonite (Cu-ETi-PILC)			108							9.3			
Fe Incorporation to Ti-pillared bentonite (Fe-PTi-PILC)			218							9.8			
Cu Incorporation to Ti-pillared bentonite (Cu-PTi-PILC)			191							8.1			
Magnetic 3-acrylamidopropyltrimethylammonium chloride intercalated bentonite	Crystal Violet	Synthetic	27.8	0.7	0.0005	7	20–300	120	50	1210	Hydrogen bonding, electrostatic interaction	OH NH	(Ain et al., 2020a)
	Anionic Congo red					5	10–250			2286			
Sulfur-doped titanium dioxide hollow spheres loaded on magnetic bentonite	Bisphenol A	Synthetic	53.63	4	0.02	7	20–110	200	Room Temperature	77.4	–	–	(Cao et al., 2020)
Bentonite-Fe/Pd	Tetracycline	Synthetic	–	–	0.009	7	20	90	–	*98%	–	–	(Gopal et al., 2020)
Iron oxide/bentonite	Diesel oil	Synthetic	–	72	0.1	6.5	50–170	180	30	54.0	Chemical bond, hydrophobic interaction, hydrogen bond	OH CO CH Si-O-Si Si-OH	(Ewis et al., 2020)
Polydopamine modified Fe_3O_4-pillared bentonite	Crystal Violet	Synthetic	27.49	4.04	0.0015	7	10–200	120	Room Temperature	1235	–	–	(Ain et al., 2020b)
Magnetic bentonite	BOD	Industrial	44.82	50.23	2	7.5–8.5	397	5 days	Room	8.26	–	–	(Khatamian et al., 2019)
	COD					5.5–6.5	1875	120	temperature	41.63	–	–	
Magnetized bentonite (APTES-Fe_3O_4/bentonite)	Methylene Blue ()	Synthetic	140.62	30.16	0.01	8	10–20	120	60	103.4	Hydrogen bond	OH Si-OH	(Lou et al., 2017)
Iron oxide/bentonite	4-nitrophenol	synthetic	–	72	0.275	11	100	120	30	96.84%	Van der Waals, hydrogen bond, π–π interaction, anion–π interaction, cation–π interaction.	-OH -FeOO- Si-OH Si-O-Si Fe—O	(Ewis et al., 2022a)

* Removal/Reduction percentage.

ultrasound. This could be attributed to the appropriate electrostatic interaction between the positively charged Fe_3O_4 NPs with the negatively charged montmorillonite surface, which leads to a good distribution of Fe_3O_4 NPs (Cottet et al., 2014; Ouachtak et al., 2020). Furthermore, Fe_3O_4 NPs are embedded in the interlayer of montmorillonite and are not restricted to the surface (Vanamudan et al., 2014).

Binders are used in the fabrication of metals oxides/montmorillonite to enhance the surface properties. Poly(vinyl) alcohol (PVA) is used as a binder due to its emulsifying and adhesive properties. Recently, a research work studied the changes of montmorillonite (MT) surface properties after covering the MT surface with PVA (Ngoh and Nawi, 2016). The SEM showed that PVA covered the voids of montmorillonite and caused the structure to become more rigid and thicker sheet-like rather than the curled up form voids that montmorillonite possess. Additionally, the pore volume and specific surface area for MT-PVAB were reduced significantly compared to raw MT. Furthermore, Titanium dioxide nanoparticles (TiO_2 NPs) were integrated into MT-PVAB to enable the composite to possess adsorptive behavior and photocatalytic activity simultaneously towards Methylene blue. The fabrication process involved sintering PVAB solution with MT followed by casting the colloidal solution onto a clean glass plate (GP) and then the deposition of TiO_2 NPs via dip-coating method to produce TiO_2/MT-PVAB/GP composite. The adsorption experiments showed that TiO_2/MT-PVAB/GP attained 93% removal of methylene blue in 45 min under dark conditions, whereas TiO_2/GP attained only 19% removal under similar conditions.

It is well-known that increasing the ionic strength for the suspension enhances the adsorption of organic pollutants when the adsorption mechanism is controlled by electrostatic repulsion and ion exchange. This is because salts such as NaCl introduces cations that stimulate compression of electric double layer around the clay mineral composite surface, which enhance the interaction between negatively charged clay mineral composite and the pollutant functional groups. This increases the clay mineral composite adsorption capacity. For instance, the adsorption of levofloxacin onto iron-pillared montmorillonite composite was not affected by the addition of NaCl. This because the adsorption of levofloxacin onto iron-pillared montmorillonite is mainly through surface complexation mechanism (Liu et al., 2015).

Temperature is one of the factors that affect the adsorbent adsorption capacity significantly as it can alter the pollutant adsorption rate before equilibrium is reached and it can affect the adsorption equilibrium of the adsorbent towards certain pollutants (Almeida et al., 2009). For organic pollutants adsorption onto montmorillonite/metal oxides, temperature does not have a generalized trend. For instance, the adsorption capacity of Ti-pillared montmorillonite at different temperatures towards several pharmaceutical compounds (amoxicillin (AMOX), imipramine (IMP), diclofenac-sodium (DIF-S), and paracetamol (PCM) did not have the same trend (Chauhan et al., 2020). In fact, the adsorption of IMP and DIF-S increased with temperature, while the adsorption of AMOX and PCM decreased with temperature. This is because the molecular properties of these pharmaceutical compounds differ. IMP and DIF-S have an electronegative center in their molecules, which facilitates the formation of hydrogen bonds with water molecules in the aqueous phase. Consequently, the high temperature causes dehydration (the hydrogen bonds weaken) and makes the molecules more planar with a higher dipole moment, which facilities their diffusion through micropores of montmorillonite composite. On the other hand, the diffusion of AMOX and PCM remains constant or decreases due to added dissolutions.

Interestingly, metal oxide/montmorillonite composites can possess a spherical shape resulting in a more stable structure and larger specific surface area and pore volume compared to flat sheet structure. In a recent work, spherical Mt. decorated with silver nanoparticles (Ag@SMT) was fabricated using spray-drying process (Wang et al., 2019). Generally, the morphology of spherically shaped particles generated from spray-drying is more stable compared to flat-sheet adsorbents. This is confirmed by the SEM images, which indicated that after the deposition of silver nanoparticles on the surface of SMT, its morphology was not affected significantly. Moreover, SMt attained a larger specific surface area and pore volume compared to raw Mt. However, the deposition of Ag NPs caused a reduction in SMt specific surface area and pore volume due to the occupation of a large amount of Ag NPs on SMt surface. Even though Ag@SMt composite possesses a lower removal for methylene blue (83%) compared to SMt (99.2%), the composite exhibit excellent catalytic performance towards methylene blue compared to individual Ag NPs and SMt. Besides, the composite exhibits 100% catalytic reduction performance over 5 cycles. Table 2 summarizes the adsorption performance of montmorillonite /metals and metal oxides composites towards organic water pollutants.

3.1.3. Kaolinite/metals and metal oxide composites

A limited number of studies have undergone the exploration of kaolinite/metals and metals oxides for organic water pollutants removal. Fei et al. (2020) fabricated Fe_3O_4/kaolinite nanocomposite for methylene blue and crystal violet removal. The SEM images revealed that when Fe_3O_4 content in the nanocomposite was 7%, Fe_3O_4 NPs were uniformly distributed on kaolinite surface without significant agglomeration. However, the agglomeration of nanoparticles was obvious when Fe_3O_4 content in the nanocomposite was 30%. This indicates that the ratio of Fe_3O_4 NPs in composites plays a significant role in the composite adsorptive behavior besides the adsorbent surface morphology. Moreover, 7% Fe_3O_4/kaolinite nanocomposite attained an adsorption capacity (q_m) of 42.3 mg/g and 138.5 mg/g for Methylene blue and Crystal violet, respectively. On the other hand, raw kaolinite and Fe_3O_4 NPs attained a qm value of 13.8 mg/g and 10.9 mg/g for methylene blue, respectively, While they attained qm value towards crystals violets of 14.3 mg/g and 25.5 mg/g, respectively. Guo et al. (2011) synthesized molecularly imprinted polymer based on kaolinite/Fe_3O_4 (MMIPs) composite for bisphenol A removal. Generally, the surface imprinting technique produces a 3D cross-linked polymer network that has prominent selectively towards a specific pollutant. In this work, kaolinite/Fe_3O_4 has been used as a supporter. Despite the fact that MMIPs attained a bisphenol A removal capacity of 142.9 mg/g, the adsorption capacity of kaolinite/Fe_3O_4 was not investigated towards bisphenol A in order to signify the need for MMIP synthesis. Moreover, the specific surface area for MMIPs composite was higher than kaolinite/Fe_3O_4 composite, while the pore volume for MMIPs was lower than kaolinite/Fe_3O_4 composite. The specific surface area and pore volume cannot altogether confirm the enhancement in adsorption capacity of MMIPs compared to kaolinite/Fe_3O_4 composite. Besides, the thermal stability for MMIP composite was less than kaolinite/Fe_3O_4. Therefore, investigation of the adsorption capacity for the same adsorbent at identical conditions needs to be carried out to signify the use of MMIPs for bisphenol A removal.

The ionic strength can influence the adsorption capacity of the kaolinite/metal oxides composites considerably towards dyes by influence its uptake mechanism. Generally, increasing the ionic strength can diminish the attraction when the adsorption process is controlled by electrostatic attraction; while it increases the attraction in case the adsorption process is controlled by electrostatic repulsion. In one of the adsorption studies, it is reported that the adsorption of Congo red increases as the ionic strength (concentration of NaCl) increases. This is attributed to the increase in the attraction between the non-polar groups of Congo red with non-polar group of the metal oxide/kaolinite composite, which indicates the presence of hydrophobic interaction. The presence of salt prevented the intermolecular replusion between dye and the composite. On the other hand, the ionic strength did not influence the adsorption of Deoxycycline, which indicates that hydrophobic interaction may not be responsible for the adsorption process (Olusegun and Mohallem, 2020).

The presence of natural organic matter (NOM) may influence the adsorption process (Wang et al., 2020a). However, Olusegun and Mohallem (2020) reported that the presence of humic acid (HA) did not affect the adsorption of Congo red and Deoxycycline onto Kaolinite

Table 2
Adsorption performance of montmorillonite/metals and metal oxides composites towards organic water pollutants.

Composite	Pollutant	Type of water	Specific surface area (m^2/g)	Magnetic saturation (emu/g)	Experiment conditions					Adsorption capacity q_{max} (mg/g)	Mechanism	Surface functional groups	Ref.
					Dosage (g)	pH	Initial concentration (mg/L)	Time (min)	Temperature (°C)				
Iron oxide/montmorillonite	Methylene Blue	Synthetic	118.1	–	0.1	5.5–7.5	100–1000	240	35 45 60	69.1 71.1 70.6	Electrostatic interaction	Si-O OH	(Cottet et al., 2014)
Iron modified montmorillonite	Crystal Violet	Synthetic	46	–	0.15	3	100–1000	1440	25	122.4	–	–	(Guz et al., 2014)
Iron-pillared montmorillonite	Levofloxacin	Synthetic	127	–	0.025	7	20–100	2880	25 35 45	48.6 65.0 56.7	Surface complexation	Metal atom centers	(Liu et al., 2015)
Iron oxide/activated montmorillonite	Methylene Blue	Synthetic	147.92	–	0.5	7	100–1000	25	20	106.4			(Chang et al., 2016)
Iron oxide/montmorillonite	Rhodamine B	Synthetic	39.08	21.8	1.0	5.5	50–350	25	25	209.2	Electrostatic interaction, hydrogen bonds, lewis interaction	OH Fe—O Si—O Al-O	(Ouachtak et al., 2020)
TiO_2 polyvinyl alcohol Montmorillonite-	Methylene Blue	Synthetic	74.99	–	*on glass plate	7	10	45	25	*93%	–	–	(Ngoh and Nawi, 2016)
Iron oxide-montmorillonite	Enrofloxaci	Synthetic	64.78	27.57	100 mg/L	6.85	–	720	25	162.9	–	–	(Peng et al., 2019)
Sodiumeicosenoate(SEIA, anionic surfactant) and Cetyltrimethylammoniumchloride modified magnetic montmorillonite (Fe_3O_4-CTMAC/ SEIA-Mt)	Methylene Blue	Synthetic	–	16.91	0.01	Neutral	10–250	180	25	242.4	Physical adsorption (weak forces of attraction)	O-C=O Al(Mg)-OH Si-O	(Rahmani et al., 2020b)
Spherical montmorillonite-supported nano-silver	Methylene Blue	Synthetic	45.3	–	0.02	6.5	100	400	–	*83%	–	–	(Wang et al., 2019)
Ti-pillared montmorillonite	Amoxicillin	Synthetic	216	–	0.005	7	0–100	60	25 35 45	4.5 3.6 2.8	–	–	(Chauhan et al., 2020)
	Imipramine							120	25 35 45	81.0 85.6 91.5			
	Diclofenac-sodium							60	25 35 45	15.5 19.3 23.8			
	Paracetamol							60	25 35 45	22.1 15.0 10.2			
Fe- Acidified organic montmorillonite	Nitrobenzene	Synthetic	117.4	–	0.02	4	0–100	1440	25	10.15	Hydrophobic interaction	Si-OH =Fe-OH	(Yang et al., 2020)

supported $CoFe_2O_4$ nanoparticles. This is attributed to the electrostatic repulsion between the negatively charged surface of the composite and HA. Consequently, HA could not block the active sites of the composite.

There are attempts to synthesis multifunctional kaolinite/metals and metals oxides composites that are able to degrade and adsorb the organic pollutant simultaneously. For instance, crystal violet removal was investigated using multifunctional kaolinite-supported nanoscale zero-valent iron (K-nZVI) and iron-manganese oxide coated kaolinite (IMK) (Chen et al., 2013; Khan et al., 2015). K-nZVI attained a removal capacity of 181.81 mg/g at 45 °C, whereby IMK attained a removal capacity of 20.643 mg/g at 40 °C, which is mainly attributed to the combined catalytic reduction and adsorption behavior of K-NZVI. Table 3 summarizes the adsorption performance of kaolinite /metals and metal oxides composites towards organic water pollutants.

It is worth noting that most work has been done on clay minerals/metal oxide composites rather than clay minerals/metals. In our opinion, it is because of metal oxides strong magnetic property compared to metals, which facilitates the composite separation from aqueous solution through an external magnet. In addition, in many cases, the adsorption capacity tends to increase with the increase in the specific surface area (Zeng et al., 2009). As shown in Tables 2-3 Clay minerals/metals oxide have a larger specific surface area compared to clay minerals/metals. For instance, the specific surface area of 7% Fe_3O_4/kaolinite is greater than the specific surface area of kaolinite-supported nanoscale zero-valent iron (Table 3). Similarly, the specific surface area for iron oxide/montmorillonite is greater than the specific surface area of iron modified montmorillonite (Table 2). This indicates that clay minerals/metals oxide might have a better adsorption capacity compared to clay minerals/metals.

3.2. Clay/minerals-carbohydrate composites

Carbohydrates polymers, such as chitosan and alginate are natural occurring materials that exist in different cell structures (Ansari et al., 2020). Chitosan is a type of polysaccharide, bioactive polymer that exists in living organisms. It is rich with amino groups as it consists of glucosamine and acetyl glucosamine units (Acosta-Ferreira et al., 2020). It is widely available in marine organisms such as shrimp, algal cell membrane and mollusks skeletons. Chitosan is a special type of polymeric material owing to its environmentally friendly nature, biodegradability, biocompatibility, availability in nature, anti-bacteria activity, and cost-effectiveness (Morais da Silva et al., 2020; Sadiq et al., 2020). Subsequently, chitosan is utilized extensively as an adsorbent in wastewater treatment. In particular, the existence of free amino and hydroxyl active groups enhances the chitosan adsorption character. However, chitosan has a relatively low specific surface area, low mechanical strength and tends to dissolve or form a gel in slightly acidic media, which limits its application as an adsorbent in wastewater treatment (Morais da Silva et al., 2020; Marrakchi et al., 2020). In order to enhance chitosan physicochemical properties and stability, chitosan is combined with other adsorptive materials such as clay minerals (Upadhyay et al., 2021). To the best of the author's knowledge, the literature research has showed that bentonite and montmorillonite are the most used clay minerals with chitosan and no research was done on kaolinite/chitosan composites.

3.2.1. Bentonite/carbohydrate composites

Extensive number of studies involved the synthesis of bentonite/chitosan composite for organic water pollutants removal including g dyes, antibiotics, and real industrial wastewater. The studies showed that bentonite/chitosan composite has a high adsorption capacity. The removal of Amino Black 10B dye using cross-linked chitosan/bentonite (Liu et al., 2015b), Zr(IV) surface-immobilized cross-linked chitosan/bentonite (Zhang et al., 2016a), crosslinked quaternized chitosan/bentonite composite (Zhang et al., 2016a) and quaternized chitosan coated bentonite (Chen et al., 2016) has been studied. Among the indicated composites, crosslinked quaternized chitosan/bentonite composite attained the highest adsorption capacity of Amino Black 10B. This is due to the use of highly positive quaternized chitosan, which is one of the chitosan derivatives. In addition, the slight difference in the adsorption capacities of quaternized chitosan coated bentonite (925.9 mg/g) and crosslinked quaternized chitosan/bentonite composite (1041.6 mg/g) at 45 °C could be attributed to the variation in preparation conditions and type of chemical used.

The composite specific surface area and pore volume may not play a critical role in determining the decrease or increase in the adsorption capacity of the composite compared to its individual components. This is attributed to the fact that carbohydrates polymers tend to block the porosity of bentonite, which causes a reduction in specific surface area and pore volume, yet the adsorption capacity of the composite is enhanced significantly. For instance, Oussalah et al. (2018) fabricated alginate/natural bentonite (A/B) composite for methylene blue removal. The study revealed that A/B composite attained an adsorption capacity of 1168.44 mg/g, which is greater than the adsorption capacity attained by bentonite clay (385.25 mg/g).

The mechanical strength is expected to enhance for bentonite/chitosan composite relative to bentonite and chitosan. Dotto et al. (2016) reported that chitosan/bentonite composite attained a higher mechanical strength compared to pure chitosan. In another study, cross-linked chitosan coated bentonite (CCB) was found to have high thermal stability compared to native bentonite and chitosan. In addition, CCB exhibited porous and irregular surface, whereas, chitosan seemed fibrous, regular and loose (Vithalkar and Jugade, 2020).

Huang et al. (2016) investigated the removal of congo red dye using crosslinked chitosan immobilized bentonite (CCS/BT). The composite showed an adsorption capacity of 500 mg/g compared to raw chitosan (CCS) that attained an adsorption capacity of 404.9 mg/g. Moreover, the effect of pH on the adsorption performance was investigated. The results showed the adsorption capacity of both adsorbents decreases as the congo red solution pH increases. This could be attributed to the negatively charged CCS/BT surface above the point of zero charge (pH_{PZC}) and the existence of congo red dye anions in alkaline medium, which increases the electrostatic repulsion as well as the competitive adsorption of abundant OH^- ions. Similar findings were reported by Abukhadra et al. (2019a) where the adsorption of congo red dye using bentonite/chitosan@cobalt oxide composite decreased as the pH increased. The mentioned composite was used to remove congo red in distilled, tap, ground and sewage water with an initial concentration of 100 mg/L. The composite attained a removal of around 98%, 97%, 91% and 87%, respectively. In another work, chitosan immobilized bentonite was able to reduce COD concentration of wastewater from 10,179 mg/L to 1730 mg/L (Abukhadra et al., 2019a). This confirms that the composite can be utilized in real industrial wastewater treatment.

The water matrices influence the adsorption process significantly, which is essentially due to the presence of other water pollutants that compete to be adsorbed. In all reported studies the adsorption of specific pollutant onto chitosan/bentonite composites is higher in distilled water > tap water > groundwater > industrial wastewater > sea water (Abukhadra et al., 2019a; Mahmoud et al., 2020). It is worth noting that the reactivity of the interfering ions contributes to the adsorption process. For instance, Na^+ and K^+ react with the carboxylic groups that exist in organic pollutants to form their sodium or potassium salts rather than interacting with the composite. Other ions such as Mg^{2+} and Ca^{2+} may reduce the adsorption of some organic pollutants by binding with the composite active surface functional groups (Mahmoud et al., 2020).

It is crucial to mention that the optimum dosage is influenced by the type of the organic pollutant rather than the physicochemical properties of the composite only. For instance, the optimum dosage required for removal of levofloxacin and ceftriaxone using nanotitanium oxide/chitosan/nano-bentonite were about 1.5 g/L and 10 g/L, respectively (Mahmoud et al., 2020). This indicates that the properties and the structure of the organic pollutant influence its uptake by an adsorbent.

Table 3
Adsorption performance of kaolinite/metals and metal oxides composites towards organic water pollutants.

Composite	Pollutant	Type of water	Specific surface area (m^2/g)	Magnetic saturation (emu/g)	Experiment conditions					Adsorption capacity q_{max} (mg/g)	Mechanism	Surface functional groups	Ref.
					Dosage (g)	pH	Initial concentration (mg/L)	Time (min)	Temperature (°C)				
Kaolinite supported $CoFe_2O_4$ nanoparticles	Deoxycycline	Synthetic	24	–	0.016	6	0–600	720	25	547	Hydrogen bond, n-π interaction	C=O SO_3-H C-N	(Olusegun and Mohallem, 2020)
									30	543			
									40	541	Hydrogen bond, n-π interaction		
									50	520			
									60	497	Hydrogen bond		
	Congo red				0.01			600	25	240	Hydrophobic interaction, hydrogen bond		
									30	246			
									40	389			
									50	396			
									60	400			
7% Fe_3O_4/kaolinite	Methylene Blue	Synthetic	21.3	–	0.05	7	25–400	90	–	42.3	Electrostatic interaction, van der waals force, hydrogen bond	OH Al-O-Si Al-OH	(Fei et al., 2020)
	Congo red									138.5			
30% Fe_3O_4/kaolinite	Methylene Blue	Synthetic	9.1							14.3			
	Congo red									27.5			
Kaolinite-supported nanoscale zero-valent iron	Crystal violet	Synthetic	19.84	–	0.06	3.09–5.50	50–300	30	25	129.9	–	–	(Chen et al., 2013)
									30	144.9			
									35	166.7			
									45	181.8			
Iron-manganese oxide coated kaolinite	Basic fuchsin	Synthetic	–	–	0.1	7	20–40	50	30	8.9	–	–	(Khan et al., 2015)
									35	9.5			
									40	10.4			
	Crystal violet				0.075		35–50		30	20.0			
									35	20.6			
									40	20.6			
Magnetic molecularly polymers (MMIPs) based on kaolinite/Fe_3O_4	Bisphenol A	Synthetic	142.90	1.98	0.01	3	20–400	720	25	142.9	–	–	(Guo et al., 2011)
									35	123.5			
									45	113.6			
Magnetic non-imprinted polymers based on kaolinite/Fe_3O_4			150.8	–					25	112.4			
									35	79.4			
									45	68.0			

From our point of view, the chemical structure of Ceftriaxone compared to levofloxacin is very complex, thereby it required a higher amount of dosage.

It is important to carry out a column study to evaluate the adsorbent performance in treating a large volume of wastewater. Vithalkar and Jugade (2020) studied the performance of cross-linked chitosan-coated bentonite towards crystal violet removal. The study was carried out in two glass columns with a length of 20 cm and an internal diameter of 1.0 cm. The column was filled with 500 mg of the composite up to a height of 4 cm to treat 10 mg/L and 20 mg/L of crystal violet solution. The results suggested that around 2080 ml and 1070 ml of water can be treated for inlet crystal violet solution concentration of 10 mg/L and 20 mg/L, respectively. Table 4 summarizes the adsorption performance of bentonite /chitosan composites towards organic water pollutants.

3.2.2. Montmorillonite/carbohydrate composites

Montmorillonite/carbohydrate composites were fabricated and used to remove organic dyes in several studies (Kittinaovarat et al., 2010; Wei et al., 2019; El-Kousy et al., 2020; Mahmoud et al., 2020). The studies show montmorillonite/chitosan composite shows a lamellar structure with strong flocculation and a rough surface. While raw montmorillonite exists in form of flakes or agglomerated flacks of various sizes. In addition, the composite exhibits higher thermal stability compared to the composite individual components. Also, the composite exhibited enhanced stability in an acidic medium with insignificant mass loss (El-Kousy et al., 2020). The adsorption capacity of montmorillonite/chitosan composite towards organic dyes was enhanced compared to raw chitosan. For instance, Kittinaovarat et al. (2010) reported that montmorillonite/chitosan composite attained an adsorption capacity towards reactive red 120 of 5.60 mg/g, whereas raw chitosan attained 4.43 mg/g. Also, El-Kousy et al. (2020) reported that montmorillonite/chitosan composite attained adsorption capacity towards methylene blue of 167.5 mg/g in 8 min, which is higher than the adsorption capacity of chitosan flakes (143.53 mg/g) that was obtained in 120 min.

Carboxymethyl chitosan (CMC) was linked to montmorillonite to remove Congo red (Zhang et al., 2020b), tetracycline and chlortetracycline (Li et al., 2019) from aqueous solution. CMC is one of chitosan derivatives that has better solubility, anti-bacteria activity, adsorption capability compared to raw chitosan (Musarurwa and Tavengwa, 2020). It is produced by carboxylation reaction to yield CMC with OH^-,NH_2 and carboxyl (-COOH) functional groups, which enhances their adsorption affinity (Shariatinia, 2018). In a recent study, Li et al. (2019) reported that carboxymethyl chitosan/montmorillonite (CMC-MT) attained an adsorption capacity of 48.10 mg/g in 2 h towards tetracycline. Whereas chitosan/montmorillonite (CHI-MT) and montmorillonite attained a tetracycline adsorption capacity of 42.45 mg/g in 4 h, and 39.31 mg/g in 24 h, respectively. This confirms that CMC can achieve high mass removal percentage compared to raw chitosan in a shorter time.

The removal of organic hydrocarbons using montmorillonite/polymer composites was also investigated. Dai et al. (2020) studied the removing of polycyclic aromatic hydrocarbons (PAHs) including acenaphthene, fluorene and phenanthrene from aqueous solution using montmorillonite sodium alginate (MSA) composite. The composite attained adsorption capacity of 1.2 mg/g, 0.9 mg/g and 2.50 mg/g towards acenaphthene, fluorene and phenanthrene, respectively. The adsorption capacity could be attributed to the porous 3D internal structure that MSA composite possesses as revealed by the SEM images and the availability of surface functional group for adsorption.

The swelling behavior of adsorbents in aqueous solution depends on the characteristics of aqueous soliton (e.g. pH, charge, ionic strength) and the adsorbent nature (e.g. hydrophilic functional groups). Generally, the swelling characteristics of montmorillonite account for its high uptake capacity towards organic pollutants as a result of the presence of active adsorption sites in the interlayer region. When it comes to montmorillonite/chitosan composites fabrication, it is important to optimize the quantity of montmorillonite integrated into chitosan network as the swelling behavior of the composite is affected significantly. In one of the adsorption studies, the highest adsorption capacity and the highest swelling ability were achieved where the montmorillonite content in the montmorillonite/chitosan composite is minimum (Vanamudan et al., 2014). This is because montmorillonite acts as a crosslinker, which causes the crosslinking density of the composite to increase when it presents in higher amounts. Eventually, this leads to a reduction in the polymer chain elasticity and restricts the penetration of water molecules into the composite. It is worth noting that swelling behavior is affected in presence of salts due to the ion effect on the physiochemical properties of chitosan. In the same study, the swelling was more after the addition of NaCl. Table 5 summarizes the adsorption performance of montmorillonite/chitosan composites towards organic water pollutants.

3.2.3. Kaolinite/carbohydrate composites

Few studies have been done on the utilization of kaolinite/carbohydrates composites for organic water pollutants removal. Table 6 shows the adsorption performance of kaolinite/carbohydrate composites towards organic water pollutants.

Chitosan contains active adsorption sites including amino and hydroxyl group that is capable to remove organic water pollutants, especially dyes. However, the main limitation of using chitosan in water pollutant removal is its high solubility in acidic environment (Jawad et al., 2020). Some types of chitosan are readily soluble in a solution with pH below 6.00 (Vårum et al., 1994). The addition of kaolinite can effectively enhance its physiochemical, structural and adsorptive properties enabling the composite to effectively adsorption pollutants in extremely acidic medium. For instance, chitosan/kaolin/γ-Fe_2O_3 composite removal capability towards methyl orange reached about 85% at pH 3.00 (Zhu et al., 2010).

Electrolytes have great influence on the adsorption process, especially dyes since they are mostly adsorbed by electrostatic interaction. Zhu et al. (2010) reported that the adsorption of methyl orange onto chitosan/kaolin/γ-Fe_2O_3 composite reduced significantly by the addition of anions. The study revealed that the adsorption was reduced with the addition of electrolyte of order: $Cl^- > NO_3^- > SO_4^{2-} > CO_3^{2-} > PO_4^{3-}$. The maximum reduction was >46%, whereas the maximum reduction was about >90%.

It is worth noting that the structural and physiochemical characteristics of kaolinite/carbohydrate changes after adsorption. Originally the composite shows a porous structure; however, after adsorption, the surface becomes smoother and flaky with some porosity. Furthermore, the elements weight percentages changes after adsorption in which new elements that belongs to the water pollutant appears (Ahmad and Ansari, 2021; Şenol et al., 2022a). Fig. 1 shows the chitosan modified hybrid *Azadirachta indica* leaves powder-Kaolinite composite structural characteristics before and after adsorption.

3.3. Clay/minerals-polymer composites

Polymeric adsorbents are extensively utilized in wastewater treatment as adsorbents due to their flexibility, high stability, and cost-effectiveness (Md. Munjur et al., 2020). In addition, some polymeric adsorbents have a relatively weak binding force with water pollutants, which allow solute recovery through regeneration methods that depend on the physiochemical properties of the adsorbate (Albatrni et al., 2019). Several studies investigated the adsorptive performance and physiochemical characteristics of clay minerals, mainly bentonite and montmorillonite, embedded into polymeric materials including cellulose (Shamsudin et al., 2019), extracellular (Ahmad and Mirza, 2018) and synthetic polymers (Azha et al., 2017).

3.3.1. Bentonite/polymer composites

The key parameters that determine the adsorption performance of

Table 4
Adsorption performance of bentonite/carbohydrate composites towards organic water pollutants.

Composite	Pollutant	Type of water	Specific surface area (m^2/g)	Experiment conditions					Adsorption capacity q_{max} (mg/g)	Mechanism	Surface functional groups	Ref.
				Dosage (g)	pH	Initial concentration (mg/L)	Time (min)	Temperature (°C)				
Crosslinked chitosan/ polyacrylicacid/bentonite	Malachitegreen	Synthetic	-	0.025	5.3	50–200	400	25 35 45	434.8 434.8 454.6	–	–	(Yildirim and Bulut, 2020)
Zr(*IV*) surface-immobilized cross-linked chitosan/bentonite	Amido Black10B	Synthetic	–	0.03	natural	50–800	480	25 35 45	418.4 584.8 588.2	Hydrogen bonding, electrostatic interaction	OH NH CO═NH_2 Amide Si—O Si-O-Si	(Zhang et al., 2016a)
Cross-linked chitosan/bentonite	Amido Black 10B	Synthetic	-	0.05	Natural	100–400	250	20 30 40	246.3 304.0 350.9	–	–	(Liu et al., 2015b)
Zr(*IV*) surface-immobilized cross-linked chitosan/bentonite	Methyl orange	Synthetic	–	0.03	Natural	100–500	300	30 40 50	438.6 438.6 425.5	–	–	(Zhang et al., 2015)
Crosslinked chitosan immobilized bentonite	Congo red	Synthetic	–	0.04	Natural	100–800	360	25 35 45 55	500 578.0 641.0 787.4	–	–	(Huang et al., 2016)
Cross-linked chitosan coated bentonite	Crystal violet	Synthetic	–	0.05	5	20–400	30	35	169.5	–	–	(Vithalkar and Jugade, 2020)
Chitosan/bentonite	Amaranth Red	Synthetic	–	0.01	2	0–500	240	25 35 45 55	362.1 324.0 289.3 271.0	–	–	(Dotto et al., 2016)
	Methylene Blue				10			25 35 45 55	496.5 496.4 441.4 407.3			
Nanotitaniumoxide/chitosan/nano-bentonite	Levofloxacin Ceftriaxone	Synthetic	16.385	0.03 0.2	4 5	5–100	10	–	90.9 90.9	–	–	(Mahmoud et al., 2020)
Bentonite/chitosan@cobalt oxide	Congo red	distilled water tap water ground water Sewage water	100.5	0.02	4	100	720	–	*98.4% *97.6% *91.3% *84.3%	Chemical bonding	OH NH C—H Si—O Al—O O-Co	(Abukhadra et al., 2019a)
Bentonite–chitosan	Humic acid	Synthetic	80	0.07	4	10–70	115	25	*91.4%	–	–	(Dehghani et al., 2018)
Chitosan immobilized bentonite	COD	Industrial	–	0.75	4.79	10,179	180	25	*83%	–	–	(El-Dib et al., 2016)
Quaternized chitosan coated bentonite	Amido black 10B	Synthetic	–	0.01	natural	100–300	300	25 35 45	990.1 1017.7 1041.6	–	–	(Chen et al., 2016)
Alginate/natural bentonite	Methylene Blue Congo red	Synthetic	11.04	0.1	6.5 7.2	25–2000 25–800	2880	24	1168.4 111.1	–	–	(Oussalah et al., 2018)
	2,4-dichlorophenol	Synthetic	–	0.01	6.4	25–500	4680	24	392	–	–	(Garmia et al., 2018)

(*continued on next page*)

Table 4 (*continued*)

Composite	Pollutant	Type of water	Specific surface area (m^2/g)	Experiment conditions				Adsorption capacity q_{max} (mg/g)	Mechanism	Surface functional groups	Ref.
				Dosage (g)	pH	Initial concentration (mg/L)	Time (min)	Temperature (°C)				
Octadecyltrimethylammonium-Bentonite/Alginate beads Hexadecyltrimethylammonium-Bentonite/Alginate beads (Fabryanty et al., 2017)	Bentonite – alginate	Crystal violet	Synthetic	56.8	0.5	–	0–300	450	185 70	601.9	–	–
Guar gum/bentonite	Crystal violet	Synthetic	5.533	0.01	7.6	5–50	300	20	167.9	Electrostatic interaction, chelation via hydrogen bond, ion exchange, surface adsorption	OH Al-OH Si-OH Si-O-Si Si—O NH	(Ahmad and Mirza, 2018)

bentonite/polymer composites are the availability of surface functional groups and the swelling capacity of the prepared composite. Herein, the composite specific surface area and pore volume do not play a critical role in determining the decrease or increase in the adsorption capacity of the composite compared to its individual components. This is attributed to the fact that polymers tend to block the porosity of bentonite, which causes a reduction in specific surface area and pore volume, yet the adsorption capacity of the composite is enhanced significantly. For instance, Shamsudin et al. (2019) reported that bentonite-zeolite-acrylic polymer-supported composite (Ben-Zeo-Acry) increased the rate of adsorption of antiseptic dye compared to acrylic polymer supported bentonite composite despite the decrease in specific surface area.

An investigation on eco-friendly polyvinyl alcohol/carboxymethyl cellulose hydrogels reinforced with bentonite composite for methylene blue adsorption has been conducted by (Dai et al., 2018). The prepared composite showed high thermal stability and excellent removing capability of methylene blue (163.93 mg/g). The introduction of bentonite to polyvinyl alcohol/carboxymethyl cellulose hydrogels caused the surface to become relatively regular without obvious particle distribution. The cross-linked structure and existence of hydrogen bonds within the composite are responsible for the enhancement in thermal stability of the composite compared to its individual components. Moreover, the composite attained good swelling ability over pH ranged from 2 to 12. The swelling ability of the said composite is a function of pH, which was controlled by the degree of –COOH group dissociation. A similar study confirmed that the degree of –COOH group dissociation and type of the composite determines the swelling ability, which might vary significantly over the entire pH values (Jana et al., 2019).

The solution ionic strength has a major effect on the adsorption capacity of bentonite/polymeric composites towards anionic and non-ionic dyes. Similar to cases discussed for kalonite/metal oxides, increasing the ionic strength (NaCl) enhanced the adsorption of anionic and non-ionic dyes into positively charged bentonite/polymer composite (polyelectrolyte-poly Epicholorohydrin dimethyl Amine/Bentonite). This can be attributed to the reduction in the repulsion forces between the negatively charged functional group of dyes, which leads to the dimerization of dyes in the aqueous solution. Also, it is possible that increasing the ionic strength causes the compression of the diffuse double layer on the composite, which facilitates electrostatic attraction and leads to an increase in the adsorption capacity (Li et al., 2010; Peng et al., 2006).

The swelling ability of the polymer is significantly affected by the addition of bentonite and graphene oxide (GO). It is reported that the addition of bentonite increased the swelling ability of the polymer due to the hydrophilic groups available on bentonite. Also, upon the addition of GO to bentonite/polymer composite increased the swelling ability further due to the availability of hydrophilic surface functional groups on GO and the formation of porous structure, which enhanced the adsorption capacity further (Dai et al., 2018).

Within natural polymeric materials, lignin is three-dimensional, low cost, ecofriendly, and able to have π- π interaction (Laurichesse and Avérous, 2014; Ge et al., 2017). A recent study conducted by Kong et al. (2019) reported that Lignin xanthate resin–bentonite clay composite attained a removal capability of doxycycline hydrochloride antibiotic 3.6 times larger than bentonite. Table 7 illustrates the adsorption performance of bentonite/polymer composites for organic water pollutants.

3.3.2. *Montmorillonite/polymer composites*

Extensive work has been done on montmorillonite/polymer composites for organic water pollutants removal including oil, dyes, and antibiotics. Table 8 shows the adsorption performance of montmorillonite/ polymer composites towards organic water pollutants. Several authors utilized montmorillonite/polymer composites for methylene blue adsorption (Mahdavinia et al., 2014; Bermúdez et al., 2018; Tong et al., 2018; Preetha and Vishalakshi, 2020; Wang et al., 2020c). Among these studies, montmorillonite supported poly(acrylamide-*co*-acrylic

Table 5
Adsorption performance of montmorillonite/carbohydrate composites towards organic water pollutants.

Composite	Pollutant	Type of water	Specific surface area (m^2/g)	Experiment conditions					Adsorption capacity q_{max} (mg/g)	Mechanism	Surface functional groups	Ref.
				Dosage (g)	pH	Initial concentration (mg/L)	Time (min)	Temperature (°C)				
Chitosan/montmorillonite	Reactive red 136	Synthetic	–	0.02	3	50–400	180	20	474.8	Hydrogen bonding, ligand exchange, van de waals, electrostatic interaction, hydrophobic interaction	OH NH Si—O $-CONH_2$	(Li et al., 2019)
Carboxymethyl-chitosan reformed montmorillonite	Tetracycline Chlortetracycline	Synthetic	119.53	0.0008	3	5–400	120	25	*95.2% *96.4%	–	–	(Li et al., 2019)
Chitosan-g-(N-vinyl pyrrolidone)/ montmorillonite	Rhoamine 6G	Synthetic	–	0.09	10	20–200		Room temperature	36.7	–	–	(Vanamudan et al., 2014)
Chitosan/modified montmorillonite beads	Reactive Red 120	Synthetic	–	0.05	5	60–140	480	30	5.6	–	–	(Kittinaovarat et al., 2010)
Chitosan/ 0.05montmorillonite	Methylene blue	Synthetic	–	0.025	8	75–400	8	25	167.5	Cation exchange, electrostatic interaction, π-π interaction between adsorbed dye molecules	OH $-NH_2$ C-O-C N-C=O Si-O-Si	(El-Kousy et al., 2020)
Chitosan/ 0.07montmorillonite				0.05					163.9			
Chitosan/0.1 montmorillonite									159.6			
Carboxymethyl chitosan hybrid montmorillonite	Congo red	Synthetic	–	0.1	7	100–500	120	25	81.8	–	–	(Zhang et al., 2020b)
Organic Montmorillonite Sodium Alginate	Acenaphthene Fuorene Phenanthrene	Synthetic	24	0.2	5–6	10	1500	25	1.2 0.9 2.5	hydrophobic interaction, wan der waals forces.	Si-O OH $-CH_2-$ NH	(Dai et al., 2020)
Montmorillonite/alginate gel	Polychlorinated Biphenyl	Synthetic	–	2.5	5.5	0.002–0.015	360	25	0.3325	–	–	(Barreca et al., 2014)
Porous cellulose derived carbon/montmorillonite	Methylene blue	Synthetic	41.8	0.05	8	60–160	60	Room temperature	138.1	Electrostatic interaction	OH CO Si—O Si-O-Al	(Tong et al., 2018)
Zr(IV) encapsulated carboxymethyl cellulose-montmorillonite	Reactive red 2 Acid orange 7	Synthetic	16.87	0.1	3	40–150	60	50	39.330 30.320	Electrostatic interaction, surface complexation, hydrogen bonding	OH Metal atom centers (Zr^{4+})	(Sirajudheen et al., 2020)
Carboxymethyl cellulose/ organic montmorillonite	Congo Red	Synthetic	–	0.1	9.6	800	–	60	171.37	–	–	(Wang and Wang, 2013)
Chitosan-montmorillonite/ polyaniline	Methylene blue	Synthetic	–	0.05	–	0–100	60	25	111	Hydrogen bond, π-π interaction	-NH -OH C=C	(Minisy et al., 2021b)

Table 6
Adsorption performance of kaolinite/carbohydrate composites towards organic water pollutants.

Composite	Pollutant	Type of water	Specific surface area (m^2/g)	Experiment conditions				Adsorption capacity q_{max} (mg/g)	Mechanism	Surface functional groups	Ref.
				Dosage (g)	pH	Initial concentration (mg/L)	Time (min)	Temperature (°C)			
Tripolyphosphate-crosslinked chitosan–kaolin	Auramine O	Synthetic	–	0.05	7.5	10–1000	1440	25	35.7	electrostatic interaction, surface complexation	-OH NH2 C—N Si-OH Al(OH)3 Si-O-Si	(Şenol et al., 2022b)
Chitosan modified hybrid *Azadirachta indica* leaves powder-Kaolinite	Congo red Methylene blue	Synthetic	–	0.015	6 7	20–100	240 180	30	104.6 99.01	electrostatic interaction, hydrogen bond, electrostatic attraction, ion exchange	SiO -NH2 -OH -OH COO- CO-	(Ahmad and Ansari, 2021)
Alginate-kaolin-graphene	Methylene blue	synthetic	–	15 g/L	5	2.5	180	room temperature	94.94%			(Nigiz, 2019)
Chitosan/kaolin/γ-Fe_2O_3	Methyl orange	synthetic	–	0.05	6	20	180	37	71%	electrostatic attraction	–	(Zhu et al., 2010)

acid) hydrogel attained the maximum adsorption capacity of 717.5 mg/g within 20 min using only 0.1 g of adsorbent (Wang et al., 2020c). In addition, the prepared composite possessed a reticular macroporous structure, which enables methylene blue molecules to enter and interact with the active sites available for adsorption. Hence, this structure would also decrease the adsorption equilibrium time due to its open-accessed structure and the availability of a wide number of active sites. Interestingly, the temperature does not influence the methylene blue removal using the said adsorbent. This is attributed to the 3D network structure the composite possesses, which provides easy access for methylene blue without the need to increase methylene blue diffusion rate by increasing the operating temperature. Another study confirms that the porous structure of cellulose-derived carbon/montmorillonite (CMt) was responsible for rapid and high methylene blue adsorption even at higher initial methylene blue concentration (e.g 140 ppm) (Tong et al., 2018). The composite attained a specific surface area of 41.8 m^2/g, meanwhile, acid-activated montmorillonite attained 39.5 m^2/g. The pore size of the composite was also higher than acid-activated montmorillonite. The increase in pore size could be attributed to the introduction of carbonaceous materials into the interlayer region, destroying some main basal spacing of montmorillonite and causing the formation of new mesopores on the composite. These factors resulted in increase in the adsorption capacity of CMt composite to be 138.1 mg/g compared to an adsorption capacity of 116 mg/g using acid-activated montmorillonite. The mentioned studies proved the high removal capabilities of various montmorillonite/polymer composites, which can be achieved in a short time. However, not all montmorillonite/polymer composites can achieve high removal capability in a short time. A study showed that sodium montmorillonite/ureasil-poly (oxyethylene) (CPN) nanocomposite reached equilibrium time in 58 h with a 69% methylene blue removal (Bermúdez et al., 2018). This is due to the electrostatic repulsion between methylene blue and CPN surface. However, the composite exhibits a high macroscopic swelling capacity (44%).

The Incorporation of montmorillonite into carboxylic containing polymeric composite may increase the swelling ratio due to the existence of -OH groups that react with -OH and -COOH groups exist on the polymeric chain. Consequently, the degree of the physical crosslinking in the polymeric chain is reduced leading to relaxation of polymeric network and enhance the water absorbency. Furthermore, the swelling behavior of montmorillonite/polymeric composite is affected by the pH. For montmorillonite/carboxylic containing polymeric composite, under basic conditions, the attraction of the surface functional groups (carboxylic and quaternary ammonium groups) to each other results in a shrinkage of the polymeric network, hence lower swelling ratio is observed. On the other hand, at neutral pH conditions, the electrostatic repulsion of carboxylic groups leads to the expansion of polymeric network leading to higher swelling (Preetha and Vishalakshi, 2020). The diffusion models showed that the highest swelling rate was observed at the neutral pH.

The removal of organic hydrocarbons using montmorillonite/polymer composites were investigated. For instance, the adsorption of motor oil and dodecane oil using montmorillonite/polyvinyl alcohol/sodium dodecyl sulfate aerogel were studied (Rotaru et al., 2014). The results reveal that the composite attained high removing capability of motor oil (25.84 mg/g) and dodecane oil (23.6 mg/g). The high adsorption capacity is mainly attributed to the mesopores and macropores domain as confirmed in the above-mentioned studies.

Microwave technology has attracted a great deal of interest in composites fabrication due to uniform energy distribution and lower synthesis time compared to conventional synthesis techniques. Recently, karaya gum-based montmorillonite nanocomposite was developed using microwave-assisted synthesis technique (Preetha and Vishalakshi, 2020; Ewis and Hameed, 2021). The synthesis process involved precursors stirring for 2 h followed by exposing the solution to microwave irradiation for only 2 min at 100 W power. The composite attained adsorption

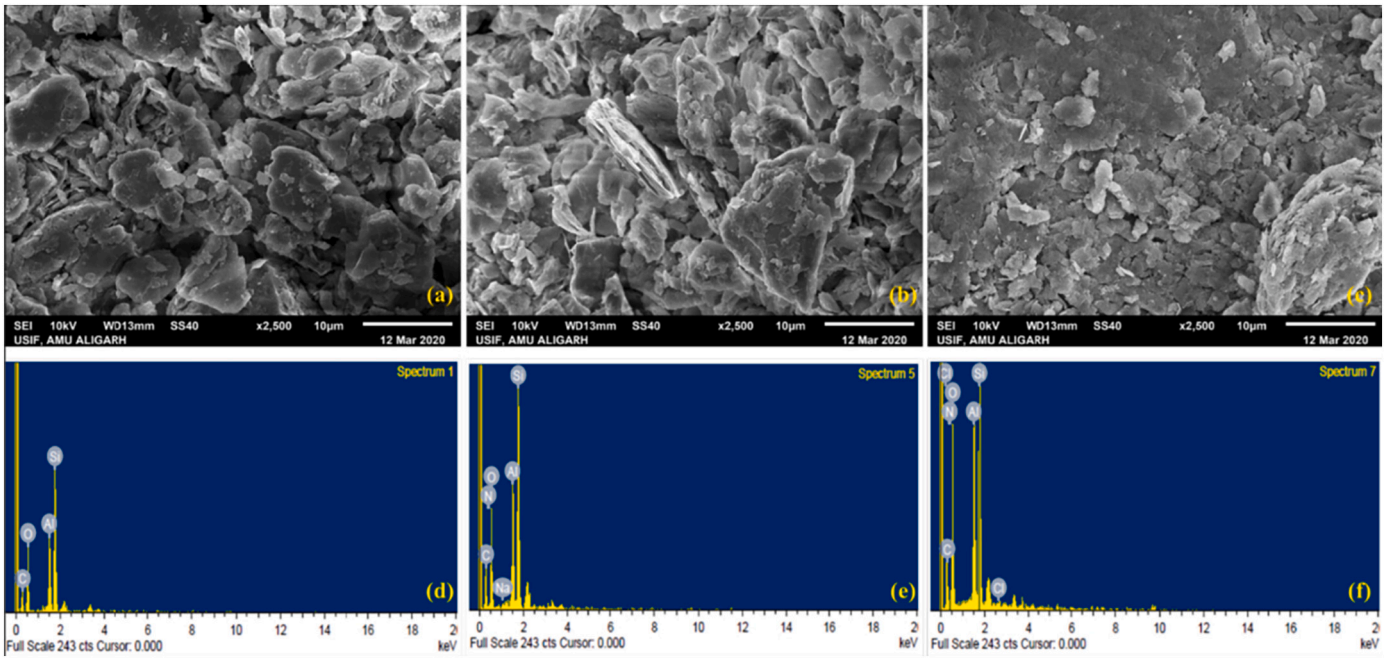

Fig. 1. SEM images of chitosan modified hybrid *Azadirachta indica* leaves powder-Kaolinite nanocomposite: (a) before adsorption; (b) after adsorption of congo red; (c) after adsorption of methylene blue dye and EDX spectra: (d) before adsorption; (e) after adsorption of congo red; (f) after adsorption of methylene blue dye adapted with permission from (Ahmad and Ansari, 2021). (For interpretation of the references to colour in this figure legend, the reader is referred to the web version of this article.)

capacity of 155.85 mg/g, 149.64 mg/g, 137.77 mg/g and 128.78 mg/g for methylene blue, toluidine blue, crystal violet and azure B, respectively. This indicates that using microwave technology in clay minerals/polymer composites synthesis reduces the fabrication cost and enriches the composites with good adsorption capacity.

3.4. Clay/minerals-carbonaceous composites

Carbon-based adsorbents such as activated carbon, carbon nanotubes, graphene etc… have outstanding characteristics including high specific surface area, high mechanical and thermal stability, controllable morphology, abundance, and high adsorption capacity (Duan et al., 2020; Gusain et al., 2020). Consequently, they are utilized extensively in wastewater treatment. Even though carbonaceous adsorbents have relatively high adsorption capacities, combing clay minerals with carbonaceous materials could enhance the overall composite adsorption performance towards some types of organic water pollutants as well as their adsorption behavior after several regeneration cycles. Over the last decade, the focus was on combing carbonaceous materials with bentonite and montmorillonite for organic water pollutants. Hence, this section discusses their adsorption behavior as well as the composites physicochemical properties.

3.4.1. Bentonite/carbonaceous composites

Few systematic studies have focused on the development of bentonite/carbonaceous composites for organic water pollutants removal. The introduction of carbonaceous material to bentonite could enhance its specific surface area, porosity, electrical conductivity and consequently enhance its adsorption capacity. Xu et al. (2019) fabricated graphene oxide/bentonite (BG) composite for toluidine blue removal. Increasing graphene oxide content enhances the specific surface area as well as the adsorption capacity; the study showed that increasing graphene oxide content from 1 wt% to 2 wt% increases the specific surface area from 56.8 m^2/g to 63.4 m^2/g. Consequently, the adsorption capacity of the composite increases from 458.7 mg/g to 471.7 mg/g. Moreover, the addition of graphene oxide to bentonite caused the formation of cracks and lamellae structure indicating the partial exfoliation of bentonite layers during the fabrication process. A similar study showed the formation of lamellae during bentonite/biochar (MSW-BC/bentonite) composite fabrication from ciprofloxacin removal, but no cracks were observed (Ashiq et al., 2019). The results showed that MSW-BC/bentonite composite attained an adsorption capacity of 286.604 mg/, while MSW-BC attained 167.610 mg/g.

The addition of carbon material to bentonite affects bentonite's interlayer spacing. For instance, after the addition of 1 wt% GO to bentonite, the interlayer spacing was improved from 1.26 nm to 1.46 nm. Furthermore, upon the addition of 2 wt% of GO to bentonite, the interlayer spacing attained a value of 1.50 nm. These results indicate an exfoliated structure (intercalation of GO within bentonite layers) (Xu et al., 2019). It is worth noting that 2 wt% GO/bentonite composite attained higher surface area, interlayer spacing compared to 1wt%GO/bentonite, which is believed to be responsible for its enhanced adsorption capacity. However, in some cases, the interlayer space may decrease upon the addition of carbon material to bentonite. Such reduction could be due to the changes to the internal structure of bentonite. Despite that, the adsorption capacity of the composite is higher compared to raw bentonite (Ashiq et al., 2019).

The performance of adsorbents in real industrial wastewater is important to investigate due to the coexistence of multiple pollutants in a relatively high concentration. A very efficient bentonite/carbon composite was developed to treat alkaline wastewater from oil refineries with chemical oxygen demand (COD) concentration of 79,834 mg/L (Liang et al., 2017). The composite was able to reduce the COD by 93% reaching a concentration of 5588 mg/L in 2 h in presence of sonication. The composite had a slightly rough surface with a curly layered structure. Table 9 summarizes the adsorption performance of bentonite/carbonaceous composites towards organic water pollutants.

3.4.2. Montmorillonite/carbonaceous composites

Extensive work has been carried out regarding the fabrication of graphene oxide/montmorillonite composite for organic water pollutants removal. An extraordinary removal capability of malachite green (1721

Table 7
Adsorption performance of bentonite/polymer composites towards organic water pollutants.

Composite	Pollutant	Type of water	Specific surface area (m^2/g)	Experiment conditions					Adsorption capacity q_{max} (mg/g)	Mechanism	Surface functional groups	Ref.
				Dosage (g)	pH	Initial concentration (mg/L)	Time (min)	Temperature (°C)				
Cationic polyelectrolyte-poly Epicholorohydrin dimethyl Amine/bentonite	Disperse Blue SBL	Synthetic	–	0.2	8.3	5–100	120	25	9.9	–	–	(Li et al., 2010)
	Vat Scarlet R				8.5	25–330			20.0			
	Reactive Violet K-3R				8.1	–			43.6			
	Acid Dark Blue 2G				7.9	–			35.1			
Acrylic polymer emulsion supported bentonite clay	Brilliant Green	Synthetic	–	0.04	3–5	50–250	300	30	52.6	–	–	(Azha et al., 2017)
Poly-epichlorohydrin-dimethylamine/bentonite	Acid Scarlet GR	Synthetic	–	0.1	7.5	70	120	30	63	–	–	(Li et al., 2011)
	Acid Dark Blue 2G				7.9				43.8			
Polyvinyl alcohol/carboxymethyl cellulose hydrogels reinforced with graphene oxide and bentonite	Methylene blue	Synthetic	–	0.03	8	50–250	140	30	172.1	–	–	(Dai et al., 2018)
Hydrogel based on katira gum-cl-poly(acrylic acid-*co*-*N*, *N*-dimethylacrylamide) incorporated bentonite (BT) nano clay	Methylene blue	Synthetic	–	0.11	8	20–80	80	50	165.3	Electrostatic interaction, hydrogen bonding	$-COO^-$ -NH Amine	(Jana et al., 2019)
	Crystal violet				7.5				158.7			
	Auramine-O				10				152.7			
Bentonite/*Co*-Poly 2-hydroxyethyl methacrylate-methyl methacrylate	5-fluorouracil	Synthetic	–	0.02	8	100–700	1440	50	369	–	–	(Abukhadra et al., 2019b)
Polymethacrylic acid grafted cellulose–bentonite	Methylene blue	Synthetic	–	1.0	6.5	0–400	240	30	371.7	–	–	(Anirudhan and Tharun, 2012)
Lignin xanthateresin–bentonite	Doxycycline hydrochloride	Synthetic	–	0.1	6	0–1000	60	25	438.8	Chemical bond, π-π interaction, hydrogen bond	OH Si-O-Si Mg-OH Si-O-Al Si-O-Mg C—O C=S	(Kong et al., 2019)

Table 8
Adsorption performance of montmorillonite/polymer composites towards organic water pollutants.

Composite	Pollutant	Type of water	Specific surface area (m^2/g)	Experiment conditions					Adsorption capacity q_{max} (mg/g)	Mechanism	Surface functional groups	Ref.
				Dosage (g)	pH	Initial concentration (mg/L)	Time (min)	Temperature (°C)				
Bacteria immobilized on montmorillonite/ polyethyleneimine	Formaldehyde	Synthetic	-	0.085	8.7	90–1100	60	25	62	–	–	(Zvulunov et al., 2019)
Polymeric Fe/Zr pillared montmorillonite	Cupper/ Ethylenediaminetetraacetic acid complex	Synthetic	145	0.05	6	10–100	60	25	16.7	Electrostatic interaction, inner-sphere complexation	Al-O Si—O Metal atom centers (Fe, Zr^{4+})	(Wu et al., 2011)
Kappacarrageenan/ sodium montmorillonite	Methylene blue	Synthetic	–	0.05	–	10–700	1440	–	344	–	–	(Mahdavinia et al., 2014)
Montmorillonite nanosheet/poly (acrylamide-*co*-acrylic acid)/sodium alginate hydrogel beads	Methylene blue	Synthetic	–	1 g/L	6.83	50–450	1400	30	407.07	Ion exchange, chemical bonding	-COOH -OH	(Wang et al., 2022)
Montmorillonite supportedpoly (acrylamide-co-acrylic acid) hydroge	Methylene blue	Synthetic	–	0.1	8	200	20	30	717.5	π-π interaction between adsorbed dye molecules, electrostatic interaction, hydrogen bond	C=O C—N C—S C=C $C=S^{+}$ $=N^{+}(CH_3)_2$ =N-H	(Wang et al., 2020c)
Polyaspartate/ montmorillonite	Methyl blue	Synthetic	10.79	0.006	2.5	–	120	25	90	Electrostatic interaction	C=C C=N S=O	(Elsherbiny et al., 2017)
Karaya gum based montmorilloni	Methylene blue Toluidine blue Crystal violet Azure B	Synthetic	–	0.05	nature	10–100	550	28	155.9 149.6 137.8 128.8	–	–	(Preetha and Vishalakshi, 2020)
Montmorilonite/ polyvinyl alcohol/ sodium dodecyl sulfate aerogel	Dodecane oil Motor oil	Pure oil	88.98	0.1	Liquid pH	Pure liquid	15 1440	25	23.6 (g/g) 25.8 (g/g)	–	–	(Rotaru et al., 2014)
Carboxymethyl cellulose-gpolyacrylamide/ montmorillonite	Malachite green	Synthetic	–	0.05	7	30–300	120	25	172.4	electrostatic interaction, hydrogen bond, π-π interaction and n-π bond.	OH COO^{-} Si-O-Si Si-O-Al	(Peighambardoust et al., 2020)
Sodium montmorillonite/ ureasil-poly (oxyethylene)	Methylene blue	Synthetic	–	0.01	–	4–10	2160	25	39.6	–	–	(Bermúdez et al., 2018)

Table 9
Adsorption performance of bentonite/carbonaceous composites towards organic water pollutants.

Composite	Pollutant	Type of water	Specific surface area (m^2/g)	Experiment conditions					Adsorption capacity q_{max} (mg/g)	Mechanism	Surface functional groups	Ref.
				Dosage (g)	pH	Initial concentration (mg/L)	Time (min)	Temperature (°C)				
Polyvinyl alcohol/carboxyl methyl hydrogels reinforced with graphene oxide and bentonite	Methylene blue	Synthetic	–	0.03	8	50–250	140	30	172.1	–	–	(Dai et al., 2018)
Graphene oxide/bentonite	Toluidine blue	Synthetic	63.4	0.05	8	200–800	1440	25	471.7	Electrostatic interaction, intermolecular interaction,	OH Si-OH Si-O-Si Si-O-Al	(Xu et al., 2019)
Biochar-bentonite	Ciprofloxacin	Synthetic	–	1 g/L	7–8	10–250	720	25	190	Electrostatic interaction,	NH NH_2^+ COO^- Si—O Al-OH	(Ashiq et al., 2019)
Bentonite/carbon	COD	Alkaline water	23.3	–	13.4	79,834	120	25	*92%	–	–	(Liang et al., 2017)
	Methylene blue	Synthetic		0.01	Natural	20–300	65	25	270.1			
Magnetic bentonite supported reduced graphene	Diesel	Synthetic	145.3	0.1	6.5	10–150	210	25	81.65	Hydrophobic interaction, electrostatic interaction, chemical bonding, π-π interaction	O-H Si-O-Si Al-O-Si Fe-O	(Ewis et al., 2022b)
Magnetic bentonite supported multiwall carbon nanotubes			156.3						77.12			

Table 10
Adsorption performance of montmorillonite/carbonaceous composites towards organic water pollutants.

Composite	Pollutant	Type of water	Specific surface area (m^2/g)	Experiment conditions					Adsorption capacity q_{max} (mg/g)	Mechanism	Surface functional groups	Ref.
				Dosage (g)	pH	Initial concentration (mg/L)	Time (min)	Temperature (°C)				
Graphene oxide – montmorillonite	P-Nitrophenol	Synthetic	–	0.1	6	0–150	60	55	60.28	–	–	(Zhang et al., 2019)
Montmorillonite/carbon	17β-Estradiol	Synthetic	50.58	0.005	7	0.2–6	1440	25	81.74	Lewis acid-base interaction, hydrogen bond, π-π interaction, electrostatic interaction, van der waals interaction, hydrophobic interaction	OH Si-O-Si Si—O C=C	(Liu et al., 2019b)
Graphene oxide/sodium montmorillonite	Malachite Green	Synthetic	230	0.004	–	15–300	20	30	1721	Electrostatic interaction, cation exchange, hydrogen bonding, π-π interaction and n-π bond	COOH OH C═O C═C C-OH	(Arabkhani et al., 2020)
Graphene oxide-montmorillonite/sodium alginate aerogel	Methylene Blue	Synthetic	266.3	0.1	5.99	30–200	60	30	150.7	Chemical bond, electrostatic interaction, hydrogen bond, π-π interaction	C=C OH Al-OH Si-O-Si COO^-	(E et al., 2020)
Montmorillonite/graphene oxide	Rhodamine B (in presence of Ni^{+2})	Synthetic	171	0.3	7	0–1000	90	30	178.6	Hydrophobic interaction, π-π interaction, electrostatic interaction	OH Si—O C═O COO^- -CH=	(Neelaveni et al., 2019)
Montmorillonite/graphene oxide/$CoFe_2O_4$	Methyl Violet	Synthetic	194.94	0.1	8	10–300	60	25	97.3	Electrostatic interaction, π-π interaction	OH COO C—O NH Si—O Al—O C═C C=O	(Foroutan et al., 2020)
Montmorillonite/graphene oxide	Methylene Blue	Synthetic	74.61	0.1	–	750	5	Room temperature	94.3%*	–	–	(Yang et al., 2019b)

Table 11
Adsorption performance of kaolinite/carbonaceous composites towards organic water pollutants.

Composite	Pollutant	Type of water	Specific surface area (m^2/g)	Experiment conditions				Adsorption capacity q_{max} (mg/g)	Mechanism	Surface functional groups	Ref.
				Dosage (g)	pH	Initial concentration (mg/L)	Time (min)	Temperature (°C)			
Kaolinite/carbon (*Carica papaya* seeds)	Methylene blue	Synthetic	–	2	6.95	1–15	2750	30	35.46	–	–	(Unuabonah et al., 2015)
Kaolinite/carbon (*Carica papaya* seeds)	2,4,6-Trichlorophenol	Synthetic	10.9	0.1	8	30–150	60	20	14.1	Electrostatic interaction, π-π interaction, Van-der Waals forces	Si-O Al-OH -NH -C-N Si-O-Si	(Olu-Owolabi et al., 2017)
Kaolinite/carbon (Pine cone)	2,4,6-Trichlorophenol	Synthetic	10						6.3			

mg/g) using graphene oxide/sodium montmorillonite composite was achieved in 20 min (E et al., 2020), which is more than triple the adsorption capacities of montmorillonite clay and reduced graphene oxide (Liu et al., 2015a; Fil, 2016). The high composite specific surface area, as well as the availability of active sites available for adsorption are responsible for the increase in the adsorption capacity. Another study reported that montmorillonite/graphene oxide attained an adsorption capacity of 641.1 mg/g within only 5 min towards methylene blue (Yang et al., 2019b). The enhancement in specific surface and the availability of active sites could be also responsible for such high adsorption. More importantly, graphene oxide in the composite played a secondary role in the adsorption process and montmorillonite contributed to the rate of adsorption by >80%.

The adsorption performance of graphene oxide/montmorillonite composite in a binary system that consists of p-nitrophenol (PNP) and lead ions (Pb^{2+}) was assessed in a recent work (Yang et al., 2019b). The study showed that in single adsorption system, the composite attained adsorption capacity of 60.28 mg/g towards PNP, and 44.96 mg/g towards Pb^{2+}. However, these values decreased in the binary system due to their competitive adsorption. The composite attained adsorption capacity of 33 mg/g and 28.02 mg/g towards PNP and Pb^{2+}, respectively. Moreover, the composite attained adsorption capacity towards PNP compared to montmorillonite and graphene oxide. This is attributed to the reduction in graphene oxide agglomeration as a result of montmorillonite addition.

Similar to bentonite/carbon composites, intercalating GO with montmorillonite results in a larger interlayer space compared to montmorillonite and GO, which is required to enhance the adsorption capacity. However, unlike the situation mentioned in (Xu et al., 2019), intercalating GO to montmorillonite required a crosslinker that acts like a barrier due to similar interlayer space of Mt. and GO (Zhang et al., 2019). Table 10 summarizes the adsorption performance of montmorillonite/ carbonaceous composites towards organic water pollutants.

3.4.3. *Kaolinite/carbonaceous composites*

The adsorption performance of kaolinite/carbonaceous composites were investigated. The chemical and physical properties of the carbon material play an important role in determining the adsorption performance of the composite, but not necessary the kaolinite structural characteristics. For instance, Olu-Owolabi et al. (2017) studied the performance of two kaolinite/carbonaceous composites for 2,4,6-trichlorophenol removal in which the carbon material originates from two different biomasses, which are *Carica-papaya*-kaolinite (CPK) and *pine-cone*-kaolinite (PCK). The results showed that the adsorption was enhanced by >250%, and 52% for CPK and PCK. In addition, the specific surface area for the composites were less than the specific surface area of pure kaolinite by >50%, yet the CEC was increased by >293% compared to pure kaolinite. Also, the study revealed that the addition of the carbon source material did not affect the structure of the kaolinite. However, the carbon material impregnated on the kaolinite surface and pores, which is responsible for the reduction in the specific surface area for CPK and PCK. Furthermore, the superior adsorptive performance of CPK compared to PCK is mainly the higher carbon content and availability of amide II groups abundantly. On pilot-scale, the use of kaolinite/carbonaceous seems a promising composite for the treatment of methylene blue from economic point of view. It is reported that 1 kg of kaolinite/carbonaceous composite would cost around $6.31, which is much lower than commercial activated carbon that costs $31.25 per kg (Unuabonah et al., 2015). Besides, the adsorption capability of kaolinite/carbonaceous composites, they attain a disinfection capacity that can adsorb and inhibit bacteria growth (Diagboya et al., 2020). Table 11 summarizes the adsorption performance of kaolinite/carbonaceous composites towards organic water pollutants.

4. Comparison of adsorbents

Adsorption technology is a cost-effective process, which can reduce the concentration of contaminants to a very low concentration making it stand out among other technologies. The selection of the suitable adsorbent is a crucial parameter when designing the adsorption unit as the adsorption process cost depends significantly on the adsorbent cost. Generally, the desired adsorbent should attain high adsorption capacity, reach equilibrium in a short time, can be re-generated and used for several cycles, have an environmentally friendly nature, high selectivity towards specific pollutants and relatively low cost.

Dye effluents are associated with paper, dye manufacturing and textile industry (Bhattacharjee et al., 2020; Ihsanullah et al., 2020). They are considered a serious source of water pollution as they possess toxic and carcinogenic properties (Sarkar and Dey, 2021). Among dyes, the removal of methylene blue using clay minerals composites has been studied extensively. The highest adsorption capacity attained was using montmorillonite supported poly(acrylamide-*co*-acrylic acid) hydrogel, which attained 717.5 mg/g adsorption capacity within 20 min for an initial dye removal of 200 mg/L. montmorillonite/graphene oxide has also achieved an adsorption capacity of 641.1 mg/g for initial dye removal 750 mg/L within 5 min only. Both adsorbents attained high adsorption capacity and have reached equilibrium in a short time. However, the recyclability, non-toxicity nature and initial methylene blue concentration in the effluent are important factors that determine which adsorbent can be used.

Treatment of oily produced water was investigated, and reported in a very limited number of studies, where different types of oil including motor, diesel and dodecane oil were used a representative for the produced water concentration. Among the above-mentioned studies related to oily produced water treatment, montmorillonite/ polyvinyl alcohol/sodium dodecyl sulfate aerogel composite showed a high adsorption capacity. Besides, the adsorbent attained high adsorption capacity through 9 cycles, had non-toxicity nature, and can be degraded biologically.

Treatment of real industrial wastewater was also studied using clay minerals composites. Among the mentioned studies, bentonite/carbon composite showed the highest ability in the treatment of alkaline wastewater (92% removal) with an initial COD concentration of 79,834 mg/L in presence of sonication. On the other hand, Fe_3O_4/ bentonite composite was able to treat wastewater with an initial COD concentration 1875 mg/L by 88% only. This indicates that the combination of bentonite with carbon source can achieve high treatment efficiency and reduce the treatment cost, as both adsorbents are inexpensive and available abundantly.

Antibiotics are a serious concern in wastewater treatment because they cannot be easily degrade biologically and tend to accumulate in the environment. Adsorption of antibiotics using clay minerals composites was investigated in limited number of studies. Within the mentioned studies, bentonite-Fe/Pd and carboxymethyl-chitosan reformed montmorillonite were highly efficient in tetracycline removal. The composite showed good adsorption capability using lower adsorbent dosage and higher initial concentration compared to bentonite-Fe/Pd.

Overall, clay and minerals composites showed excellent removal capability of various types of organic water pollutants. Bentonite/carbon composites are promising adsorbents as they showed an excellent COD reduction of highly alkaline real wastewater for several cycles. In addition, bentonite/carbon and montmorillonite/carbon composites showed an acceptable removing capability of dyes and antibiotics besides being inexpensive adsorbents. Besides their excellent adsorption capability towards organic pollutants, clay minerals and activated carbon are inexpensive. Table 12 shows the cost of commercial, raw adsorbents obtained from Sigma-Aldrich. It can be observed that clays and clay minerals are the cheapest adsorbents followed by activated carbon. It is worth mentioning that the final composite cost may doubled or tripled due to the influence of other factors such as energy cost, tax cost and labor cost. For instance, the raw materials in chitosan composites fabrication comprise about 16–25% of the total cost (Gkika et al., 2019). However, still the raw clay minerals cost is minimal, and following a cost-effective synthesis procedure considering the above-mentioned factors might result in a low-cost effective clay mineral composite.

Table 12
The cost of commercial, raw adsorbents obtained from Sigma-Aldrich.

Material	Cost (US dollar/g)
Bentonite	0.079
Kaolinite	0.12
Montmorillonite	0.25
Activated carbon	0.35
MWCNTs (98% carbon basis)	202
GO	191
Cellulose triacetate (Polymeric adsorbents)	6.02
Karaya gum (polymeric adsorbent)	0.2
Chitosan (from rom shrimp shells, ≥75% (deacetylated)	6.5
Iron oxide nanoparticles	3.36
Titanium dioxide nanoparticles	4.79
Zinc oxide nanoparticles	3.79

It is worth noting that there are several factors affecting the adsorption of organic pollutants onto clay/minerals composites and needs to be investigated to understand the adsorption process. These factors are specific surface area, pore volume, interlayer space, composite surface functional groups, composite swelling ability, solution pH, composite dosage, the ratio between clay mineral: material, initial pollutant concentration, temperature, contact time, solution ionic strength, the reactivity of interfering ions, structure of organic pollutant and hydrophobicity of the organic pollutant, water matrices and presence of NOM.

As a final conclusion, the integration of metal oxides and carbonaceous materials into clay/minerals enhances the clay/minerals surface hydrophobicity. In addition, to overcome the high dispersity of clay/minerals in aqueous solution that limits their separation, magnetizing clay/minerals are used to facilities the clay/minerals separation from aqueous solution. However, they can be used within a narrow pH range with a modest adsorption capacity. The mechanical strength and thermal stability are also enhanced for clay/minerals composites compared to the composite individual components. As for clay/minerals composites adsorptive behavior, the increase in specific surface area of the composite compared to its individual components does not always imply that the composite adsorption capacity increases. In some cases, the composite specific surface area was reduced, but attained a higher adsorption capacity compared to its individual components. This is because other factors such as surface functional groups and interlayer space play an important role in the adsorption process. Furthermore, the swelling ability of the composites contributes to its adsorption capability due to the presence of active adsorption sites within the interlayer space. The swelling capacity is greatly influenced by solution pH and ionic strength. The interlayer space can be calculated by the help of XRD analysis. However, it is important to consider that in some cases it is difficult to join two materials of similar interlayer space such as GO and bentonite; therefore, a crosslinker should be used. Also, the ionic strength plays a deceive role in the adsorption process. Increasing the ionic strength might reduce or increase the adsorption capacity. It is important to investigate the ionic strength effect on the adsorption process as it gives insights on the adsorption mechanism as discussed above. In addition, the reactivity of interfering ions should be investigated as in some cases the interfering ion might not influence the adsorption process. Finally, the solution pH affects the adsorption process significantly as it influences the structure of organic pollutant, the charge on the clay/minerals composite, and the swelling ability of the clay/minerals composite. Finally, all above-mentioned studies confirmed that increasing the ionic strength of the solution enhances the adsorption of organic pollutants when the adsorption mechanism is controlled by electrostatic repulsion and ionic exchange.

5. Adsorption mechanism

The adsorption mechanism is directly linked to the adsorbent surface properties and the nature adsorbate. The incorporation of other materials into adsorbent changes the surface properties and affects the interaction, which eventually influences the adsorption mechanism. In this review, the most common reported adsorption mechanism for clay/minerals towards organic water pollutants: chemical adsorption (e.g. covalent bond), electrostatic interaction, van der waals, hydrophobic interaction, hydrogen bonding, ion exchange, n-π interaction, surface complexation and π-π interaction. The dominate adsorption mechanism depends on the chemical properties of the organic pollutant and the structure, surface properties, and functional groups of the clay mineral composites. Furthermore, the adsorption conditions including pH, and ionic strength affect the adsorption mechanism since these conditions have the ability to alter the adsorbent surface properties. Fig. 3 shows the common adsorption mechanism of organic pollutants onto clay/minerals composites. Tables 1-11 show the interaction type of clay/minerals composites with adsorbed organic water pollutants along with the surface active functional group.

It can be seen from Tables 1-11 that electrostatic interaction is the most common adsorption mechanism. It is the ionic bond formation that includes electrostatic attraction and repulsion. It is formed between anions and cations after the process of atoms gaining and losing electrons. It is significant to examine the influence of solution pH on the clay/minerals uptake capacity. This is because the solution pH can alter the charges on the clay/minerals composite, which influence the electrostatic interaction. Fig. 2 shows the electrostatic interaction between montmorillonite/graphene oxide/$CoFe_2O_4$ and methyl violet in both acidic and alkaline medium. The main functional groups on the clay/minerals composites that contribute to the electrostatic interaction are Si—O and Al—O, which exist on the clay/minerals. The modification of clay/minerals through Fe_3O_4 NPs and acrylic acid containing polymer can add functional groups such as Fe—O, and -COO, respectively (Jana et al., 2019; Ouachtak et al., 2020). However, in some cases the electrostatic interaction through surface functional groups is insignificant despite the presence of these functional groups. This is because of the presence of other interactions provided by the composite that diminish the strength of electrostatic interaction. For instance, electrostatic interaction had an insignificant effect on the adsorption of malachite green onto graphene oxide/sodium montmorillonite composite (Arabkhani et al., 2020). Other interactions including n- π interaction and π-π interaction were responsible for the adsorption process due to the availability of benzene ring provided by graphene oxide.

Ion exchange is defined as the exchange of ions of the same charge between the adsorbent and the adsorbate. It occurs when the adsorbent adsorbs ions from the solution and releases equivalent ions back to the solution in order to maintain the solution electrical neutrality. Ion exchange is a common adsorption mechanism especially in clay/minerals-chitosan and clay/minerals-polymeric composites, which can occur through the exchange of Na^+ or ligands (Li et al., 2019; Arabkhani et al., 2020).

π-π interaction is a weak interaction that occurs between unsaturated bonds that exist on both aromatic rings in the adsorbent and the adsorbate (Chua et al., 2021). It is a common adsorption mechanism for clay/minerals-carbonaceous composites and clay/minerals-polymeric composites. The solution pH influences the π-π interaction. For instance, the adsorption of methyl violet by montmorillonite/graphene oxide/$CoFe_2O_4$ increased with increasing the initial pH, which is mainly attributed to the formation of π-π interaction (Foroutan et al., 2020). The dye molecules containing the aromatic ring can form π-π bonds with each other to form multilayers on the adsorption surface (El-Kousy et al., 2020). Furthermore, n-π interaction is a possible adsorption mechanism for clay minerals composites. The interaction can occur through functional groups including -OH, COOH and -COH, which interact with the aromatic ring to yield n- π interaction. From the FTIR spectra, the existence of C—O peak indicates the existence of such interaction at 1050 cm^{-1} (Arabkhani et al., 2020; Peighambardoust et al., 2020).

Hydrogen bonding is a type of dipole-dipole attraction in which a hydrogen (H) atom is bonded to an electronegative atom (Nitrogen (N), Oxygen (O) and Fluoride (F)). As shown in Tables 1-11, most of clay/minerals composites tend to form a hydrogen bonding with the organic pollutant, which is a very strong type of interaction.

Hydrophobic interaction refers to the interaction between nonpolar substance in a water-based system (Xie et al., 2020). Clay/minerals are generally hydrophobic, and they tend to have some degree of hydrophobicity after combining them with other materials, especially metal oxides. In fact, some studies integrate metal oxides with clay/minerals to enhance the hydrophobicity, which enhances their adsorptive capacity (Zhang and Xu, 2012; Ewis et al., 2020; Olusegun and Mohallem, 2020). Also, most of the organic pollutants have low water solubility; therefore, the organic pollutants can be easily adsorbed on the clay/minerals

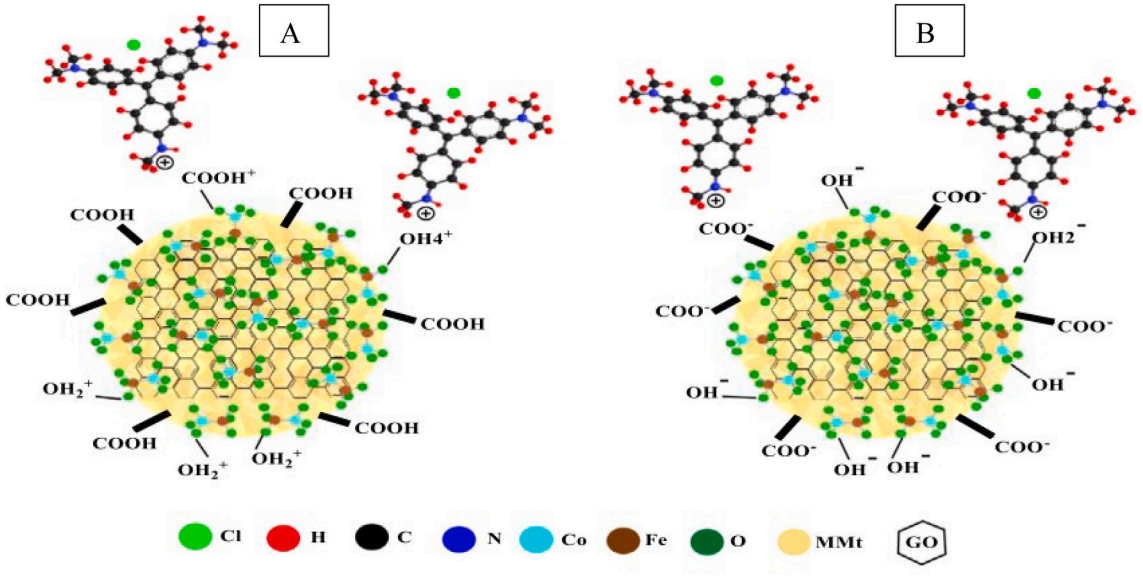

Fig. 2. The electrostatic interaction between montmorillonite/graphene oxide/$CoFe_2O_4$ and methyl violet in (A) acidic and (B) alkaline medium adapted with permission from (Foroutan et al., 2020). (For interpretation of the references to colour in this figure legend, the reader is referred to the web version of this article.)

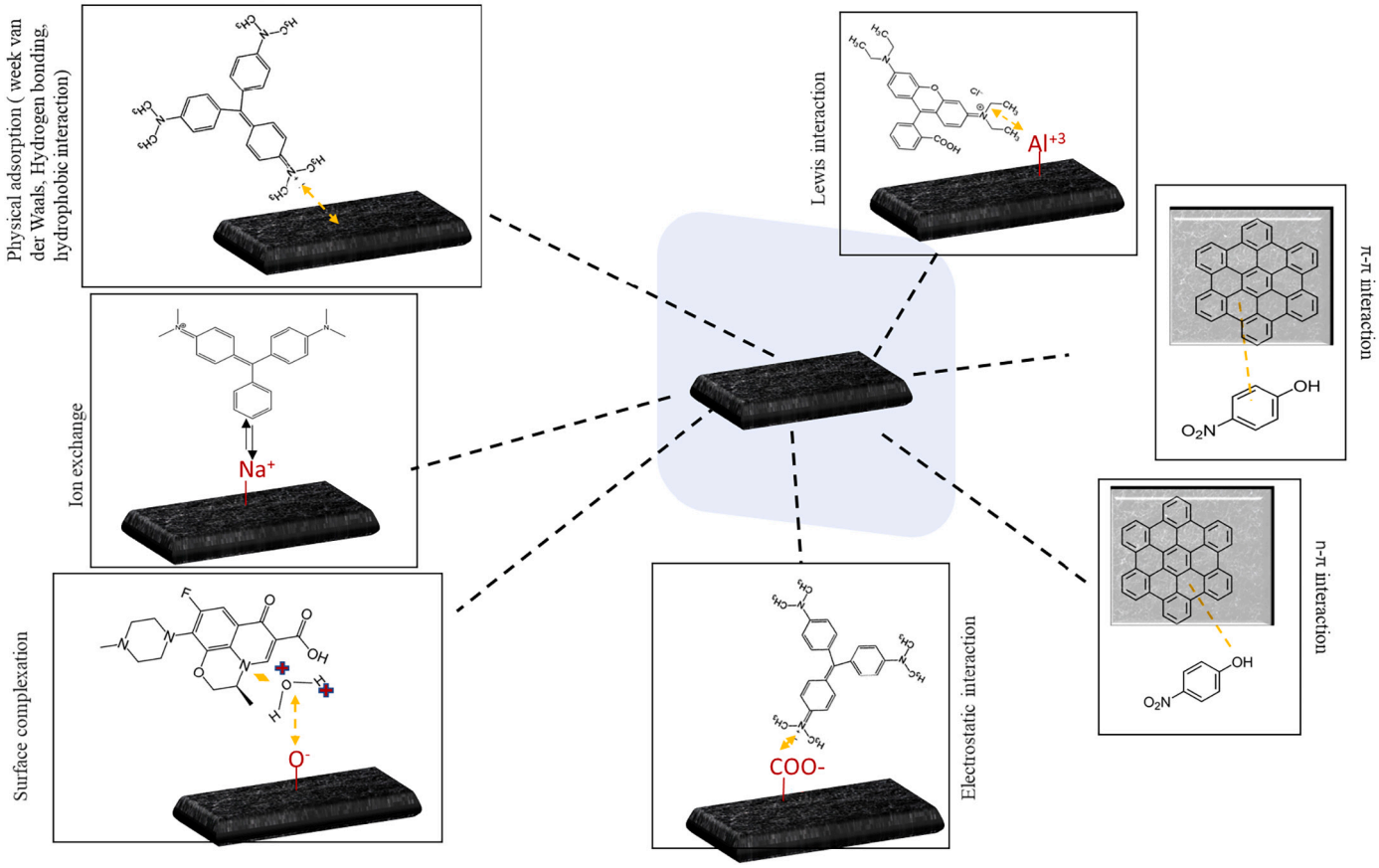

Fig. 3. Common adsorption mechanism of organic pollutants onto clay/minerals composites.

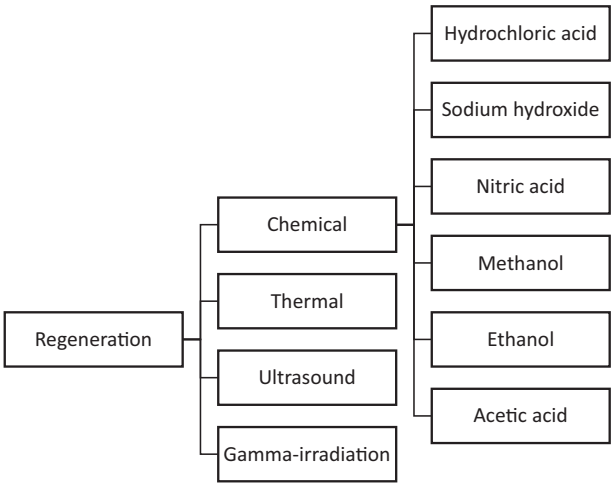

Fig. 4. The regeneration methods used for clay/minerals composites.

composite surface. The hydrophobicity is defined as n-octanol/water partition coefficient (K_{ow}/log K_{ow}). Organic compounds with a higher value of Log K_{ow} tend to be more hydrophobic; thus, can be easily adsorbed on a hydrophobic surface through hydrophobic interaction (Zhang and Xu, 2012; Olusegun and Mohallem, 2020).

Surface complexation could be involved in clay/minerals interaction with organic pollutants. Surface complexation is the electrostatic interaction of the adsorbent with the adsorbate while the adsorbate ions retain their hydration sphere (Yang et al., 2019a). It occurs as the clay/minerals composites contain metal ions with unfilled electron orbit, which may adsorb organic pollutants through coordination with the ligands. Tables 1-11 show that two studies mentioned surface complexation as the adsorption mechanism due to the existence of metal ions in their composite structure; which mainly are the adsorption of levofloxacin using iron-pillared montmorillonite composite and the adsorption of Reactive red 2 and Acid orange 7 using Zr(IV) encapsulated carboxymethyl cellulose-montmorillonite.

Lewis interaction is also proposed as an adsorption mechanism for clay/minerals towards organic water pollutants. This interaction is the existence of lone pair of electrons on the adsorbent that act as a lewis-base site to interact with the strong lewis-acid, which is the adsorbate (Xiong et al., 2020). For instance, nitrogen atom of Rhodamine B acts as a lewis base and interacted with Al^{+3}, which is the lewis acid in magnetic montmorillonite composite (Ouachtak et al., 2020). It is worth mentioning that lewis interaction depends on the pH as the solution pH affects the charges available on the composite (Liu et al., 2019a).

6. Regeneration methods

The capability of the adsorbent to be regenerated is an important aspect in the selection of suitable adsorbent. Generally, adsorbent that adsorbs high amounts of contaminant on its surface at equilibrium greater than the residual amount in water solution shows an ineffective or slow desorption/regeneration, which limits its application in water remediation (Vakili et al., 2019). Without adsorbents regeneration, the cost of the adsorption process increases, and the contaminant might be released to the environment if the spent adsorbent is disposed or stored. The contaminant recovery from the spent adsorbent allows continuous utilization of the regenerated adsorbent, and subsequently reduces the adsorption process cost (Zhang et al., 2016b; Ifthikar et al., 2018). Therefore, the use of an adequate regeneration method to recycle the

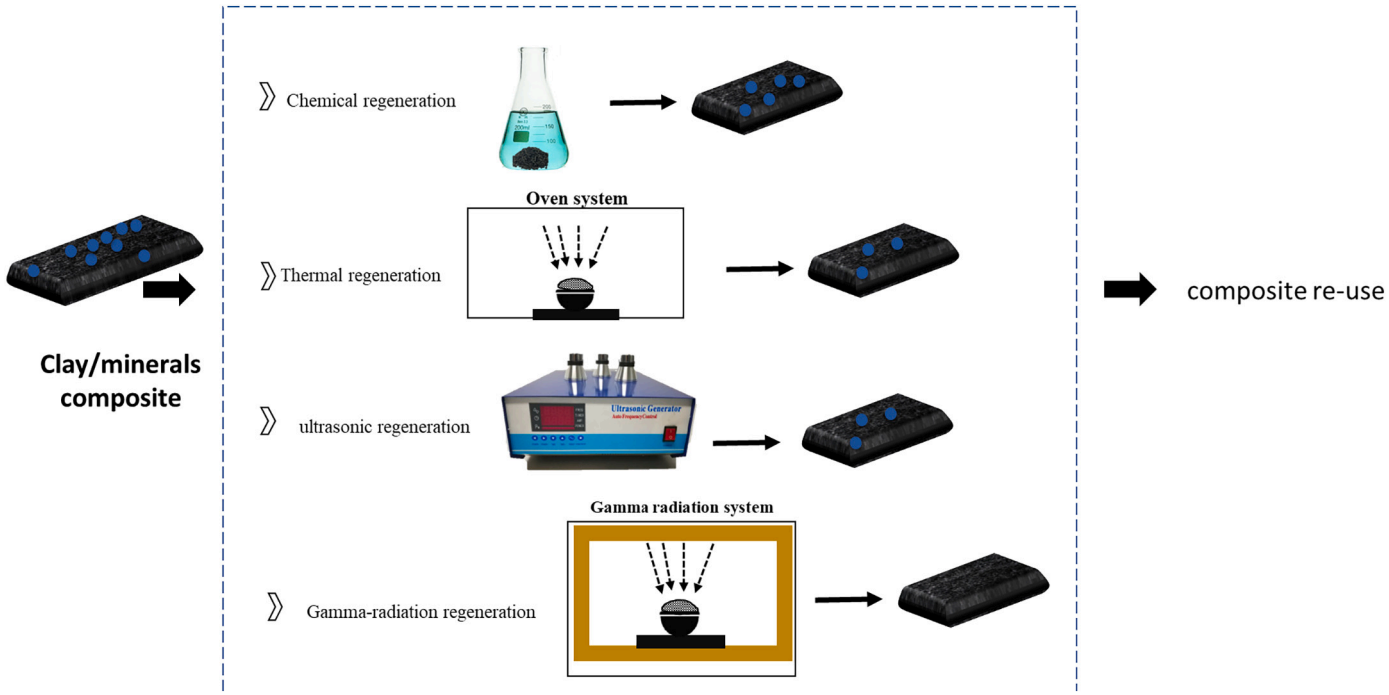

Fig. 5. The efficiency re-generation methods used for clay/minerals composites re-generation.

spent adsorbent provides substantial economic and environmental benefit. In this section, the used regeneration methods of clay/minerals composites reported in this review are identified and critically summarized. Fig. 4 shows the regenerating techniques used for clay/minerals composites along with Table 13 that summarizes the adsorption performance of clay/minerals composites towards organic pollutants after regeneration process.

6.1. *Chemical regeneration*

Chemical regeneration involves the application of specified temperature and pH value of the solvent, hence breaks the adsorption equilibrium between the adsorbent, solvent, and adsorbate. The chemical solvent can be inorganic such as hydrochloric acid (HCl) and sodium hydroxide (NaOH) or organic, such as methanol. Chemical regeneration is a suitable regeneration method for organic pollutants, which exist in a high concentration and have a relatively low boiling point. In addition, the solubility of the adsorbate in the solvent is the main factor that determines the regeneration process efficiency. The main issue associated with solvent regeneration is that the solvent can alter the adsorbent structure, which affects the adsorbent efficiency in the subsequent adsorption cycles (Momina and Suzylawati, 2020).

Extensive number of studies regenerated clay/minerals composites through chemical regeneration. Around 92% of the studies related to clay/minerals composites regeneration used chemical regeneration method. The process involves adding a predetermined amount of spent adsorbent in a solvent with specified pH under continuous mechanical stirring for several hours. After that, the adsorbent is dried and used for several cycles. The performance of the adsorbent in the subsequent cycles depends on the adsorbent physiochemical characteristics, which might be affected significantly during the regeneration process and thus affects its adsorption capacity.

Among clay/minerals composites, bacteria immobilized on montmorillonite/ polyethyleneimine (Zvulunov et al., 2019), graphene oxide/sodium montmorillonite (Arabkhani et al., 2020), and montmorillonite/graphene oxide/$CoFe_2O_4$ (Foroutan et al., 2020) attained the highest regeneration cycles as they were utilized for 10 cycles. The desorption process depends heavily on the type of solvent that is used to leach the pollutant from the adsorbent. The interaction type between the pollutant and adsorbent is a crucial parameter to consider when selecting the suitable solvent. For instance, Arabkhani et al. (2020) used different solvents (ultrapure water, acetone, methanol, acetic acid, and acetic acid/methanol) for the desorption process of malachite green from graphene oxide/sodium montmorillonite composite. The results indicated that the adsorption between malachite green and the composite is a chemisorption process. Consequently, ultrapure water was able only to desorb malachite green that is bonded physically to the composite. On the other hand, acetone, methanol, acetic acid, and acetic acid/methanol were efficient in the regeneration process due to the availability of hydrophobic CH_3 group, and hydrophilic OH and CO groups that interact with the adsorbent surface functional groups chemically and blocking the interaction between the adsorbent and malachite green. The adsorbent attained 90% removal of malachite green until the 6th cycle and then started to decrease until the 10th cycles reaching a 60% removal efficiency. It is worth noting that as the interaction complexity between the adsorbent and the adsorbate increases, the desorption efficiency decreases despite of using strong eluents such as HCl (Minisy et al., 2021a).

Thus, the regeneration efficiency is determined by the type of the interaction between the adsorbate and the adsorbent, which vary according to the type of the adsorbent and the adsorbate. An important issue to consider is that when the pollutant is strongly adsorbed on the composite surface and within its microspores, the chemical regeneration process is hindered and/or inefficient in regenerating the composite. This issue is crucial for composites that attain highly microspores structure, and strongly bonded to the organic pollutants (Kilduff and King, 1997; He et al., 2013). Thus, alternative regeneration techniques should be considered.

The solvent concentration is an important factor to consider in the regeneration process. Higher solvent concentration enhances the regeneration process. However, extremely high solvent concentration are ineffective in adsorbents regeneration (Salvador et al., 2015). Therefore, the effect of solvent concentration should be studied accordingly. For instance, a study revealed that increasing the HCl concentration from 0.001 M to 0.1 M enhances the desorption of methylene blue (Anirudhan and Tharun, 2012).

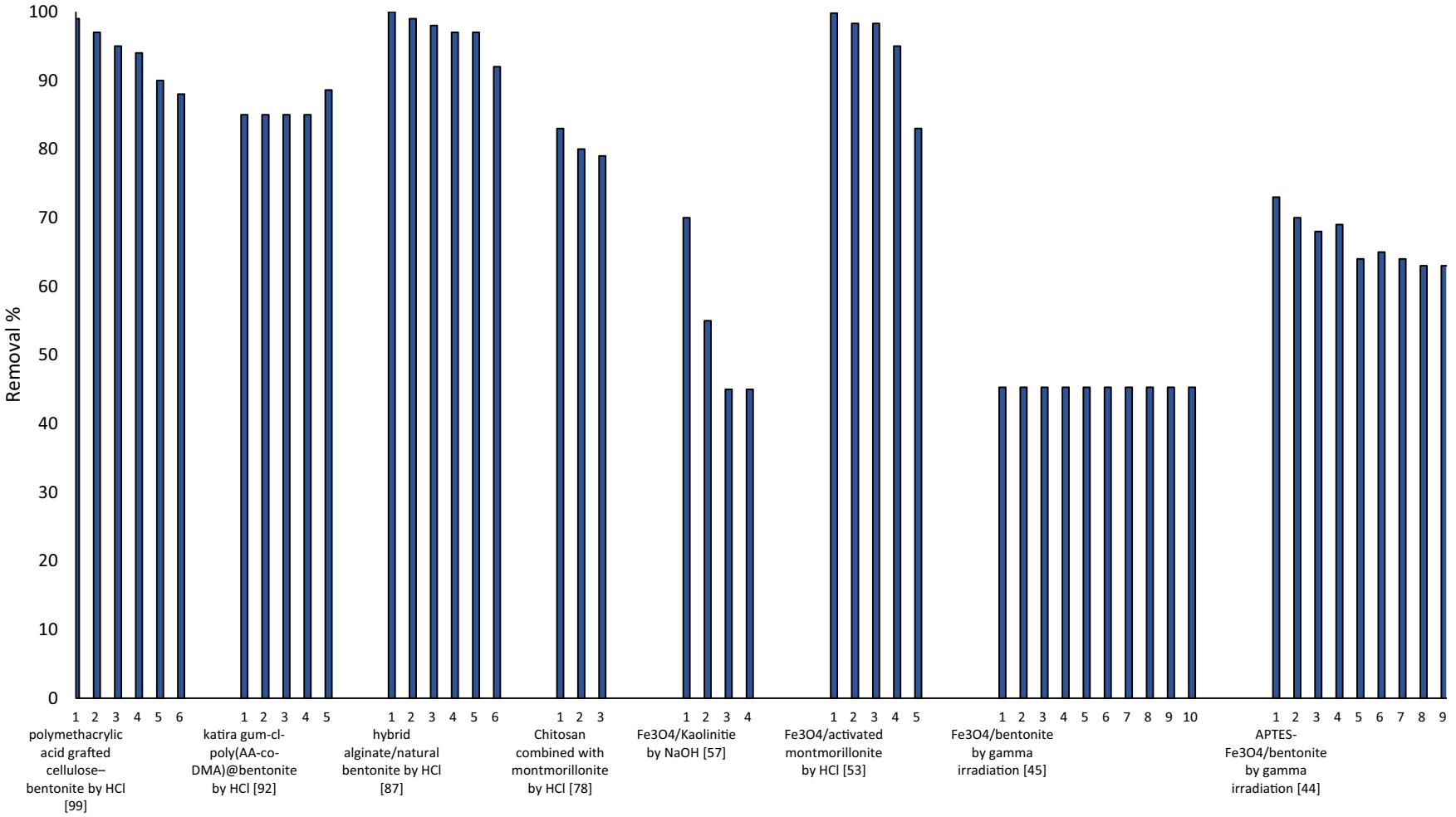

Fig. 6. The perfomance of regenerated adsorbents towards methylene blue removal. (For interpretation of the references to colour in this figure legend, the reader is referred to the web version of this article.)

Table 13
The adsorption performance of clay/minerals composites after regeneration.

Adsorbent	Pollutant	Regeneration method	No. of cycles	Adsorption%, where n = number of cycles	Ref.
Magnetic 3-acrylamidopropyltrimethylammonium	Crystal violet	Ultrasound	5	n1 = 90%, n5 = 78%	(Ain et al., 2020a)
Bentonite-Fe/Pd	Tetracycline	Chemical regeneration/ HCl	5	n1 = 99%, n5 = 45%	(Gopal et al., 2020)
Magnetized bentonite (APTES-Fe_3O_4/bentonite)	Methylene Blue	Gamma-irradiation	9	n1 = 73%, n9 = 63%	(Lou et al., 2017)
Fe_3O_4/bentonite	Methylene Blue	Gamma- irradiation	10	n1 = n10 = 45.3%	(Lou et al., 2015a)
Iron oxide/activated montmorillonite	Methylene Blue	Chemical regeneration/HCl	5	n1 = 99.8%, n5 = 84%	(Chang et al., 2016)
Sodiumeicosenoate(SEIA, anionic surfactant) and cetyltrimethylammoniumchloride modified magnetic montmorillonite	Methylene Blue	Chemical regeneration/HCl	3	n1 = 89%, n3 = 65%	(Rahmani et al., 2020b)
Ti-pillared montmorillonite	Amoxicillin	Chemical regeneration/NaOH	3	n1 = 100%, n3 = 62%	(Chauhan et al., 2020)
	Imipramine	Chemical	3	n1 = 100%, n3 = 75%	
	Diclofenac-sodium	regeneration/HNO3	3	n1 = 100%, n3 = 58%	
	Paracetamol		3	n1 = 100%, n3 = 62%	
7% Fe_3O_4/kaolinite	Methylene Blue	Chemical	4	n1 = 70%, n4 = 45%	(Fei et al., 2020)
	Congo red	regeneration/NaOH	4	n1 = 93%, n4 = 79%	
Magnetic molecularly polymers (MMIPs) based on kaolinite/ Fe_3O_4	Bisphenol A	Chemical regeneration/ methanol & acetic acid mixture	4	n1 > 85%, n4 = 79.04%	(Guo et al., 2011)
Bentonite/chitosan@cobalt oxide	Congo red	Chemical regeneration	6	n1 = 98.44%, n6 = 74.33%	(Abukhadra et al., 2019a)
Quaternized chitosan coated bentonite	Amino black 10B	Chemical regeneration/NaOH	3	n1 = 99.9%, n3 = 99.7%	(Chen et al., 2016)
Chitosan/montmorillonite	Reactive red 136	Chemical regeneration/NaOH	15	After 15 cycles the desorption ratio and regeneration ratio decreased to 61.3%, and 60.5%, respectively.	(Li et al., 2019)
Chitosan/0.05montmorillonite	Methylene Blue	Chemical regeneration /HCl	3	n1 = 82%, n3 = 79%	(El-Kousy et al., 2020)
Chitosan/0.07montmorillonite			3	n1 = 87%, n3 = 85%	
Chitosan/0.1 montmorillonite			3	n1 = 97%, n3 = 80%	
Alginate/natural bentonite	Methylene Blue	Chemical regeneration/DI water at pH = 2	6	n1 = 100%, n6 = 94%	(Oussalah et al., 2018)
	Congo red	Chemical regeneration/DI water at pH = 10	5	n1 = 85%, n5 = 45%	
Polyvinyl alcohol/carboxymethyl cellulose hydrogels reinforced with graphene oxide and bentonite	Methylene Blue	Chemical regeneration/HCl	4	*n1 = 137 mg/g, n4 = 125 mg/g	(Dai et al., 2018)
Hydrogel based on katira gum-cl-poly(acrylic acid-*co*-*N*, *N*-dimethylacrylamide) incorporated bentonite (BT) nano clay	Methylene blue	Chemical regeneration/HCl	5	n1 = n5 = 90%	(Jana et al., 2019)
	Crystal violet			n1 = 90%, n5 = 80%	
	Amino black			n1 = 91%, n5 = 83%	
polymethacrylic acid grafted cellulose–bentonite	Methylene Blue	Chemical regeneration/HCl	6	n1 = n6 = 98	(Anirudhan and Tharun, 2012)
Guar gum/bentonite	Crystal Violet	Chemical regeneration/HCl	5	–	(Ahmad and Mirza, 2018)
Organic Montmorillonite Sodium Alginate	Acenaphthene	Chemical	4	n1 = 80%, n4 = 34%	(Dai et al., 2020)
	Fluorene	regeneration/Methanol		n1 = 70%, n4 = 30%	
	Phenanthrene			n1 = 75% n4 = 33%	
Karaya gum based montmorillonite	Methylene Blue	Chemical regeneration	2	n1 = 99%, n2 = 79%	(Preetha and Vishalakshi, 2020)
	Toluidine blue			n1 = 99%, n2 = 75%	
	Azure B			n1 = 93%,n2 = 70%	
	Crystal violet			n1 = 90%, n2 = 70%	
Carbonized montmorillonite/carboxymethyl cellulose	17β-Estradio		5	*n1 = 53 mg/g, n5 = 42 mg/g	(Liu et al., 2019a)
Graphene oxide/bentonite	Toluidine blue	Chemical regeneration/ ethanol&HCl	6	n1 = 99%, n6 = 50%	(Xu et al., 2019)
Bentonite/carbon	Alkaline water (COD = 79,834 mg/L)	Carbonization	9	n1 = 68%, n9 = 90%	(Liang et al., 2017)
Graphene oxide/sodium montmorillonite	Malachite green	Chemical regeneration/ Acetic acid &methanol	10	n1 = 95%, n10 = 60%	(Arabkhani et al., 2020)
Montmorillonite/graphene oxide	Rhodamine B	Chemical regeneration/HCl	5	n1 = 99%, n5 = 85%	(Neelaveni et al., 2019)
Montmorillonite/graphene oxide/$CoFe_2O_4$	Methyl Violet	Chemical regeneration/HCl	10	n1 = 98%, n10 = 88%	(Foroutan et al., 2020)

* Adsorption capacity in mg/g.

Besides the above-mentioned factors that affect clay/minerals composites regeneration, temperature is an important factor. Temperature can increase the desorption rate by altering the adsorbate molecular activity and weakening the interaction between the adsorbate and the adsorbent (Mansour et al., 2018). In addition, temperature enhances the solubility of organic pollutants in the solvent. In most of the studies reported in this review, regeneration process is conducted at room temperature. Desorption time is another important factor. Generally, increasing desorption time increases the desorption rate since it allows more contact between the adsorbate and the solvent. After reaching the desorption equilibrium in which no more adsorbate is released into the solvent, the desorption rate remains constant and further increase in the desorption time does not affect the desorption process. The range of estimated time for clay mineral composites reported in this review varied between 3 and 24 h. However, most of these studies kept the desorption time long intentionally to ensure the system reaches the desorption equilibrium. Therefore, solvent concentration, temperature, type of interaction between the adsorbate and the adsorbent (chemical/physical interaction) and contact time are important factors in the regeneration process that need to be investigated to reach the maximal desorption efficiency.

6.2. Ultrasound sonication

In a recent study conducted by Ain et al. (2020a) 3-acrylamido propyl trimethyl ammonium chloride intercalated bentonite composite was regenerated by ultrasound technique. The process involved immersing the spent adsorbent in 10 ml of pure ethanol for an hour followed by 30 min of ultrasound sonication. The recycled composite showed a constant adsorption capacity towards Congo red over five consecutive cycles. However, there was a slight decrease in crystal violet adsorption in the second cycle by around 2%, after that the adsorption was constant until the 5th cycle. This indicates that the composite attained a good stability after several regeneration cycles.

6.3. Thermal regeneration

Thermal regeneration involves exposing the adsorbent to high temperature that is capable of destroying the bond between the adsorbate and the adsorbent. However, the thermal heat generated might reduce the adsorbent weight and alter its morphology. Besides, adsorbents that attain a low mechanical strength and low thermal stability cannot be regenerated thermally since thermal regeneration apply extremely high temperature. In clay/minerals composites, only one study used thermal regeneration. The study used carbonization of the bentonite/carbon composite at a heating rate of 5 °C/min to 500 °C for 9 cycles (Liang et al., 2017). The removal did not attain a defined pattern; however, the minimum COD removal was 46,942 mg/L for an initial COD concentration of 79,834 mg/L. Despite the high removal efficiency over the entire regeneration cycles, the composite morphology and physiochemical structure after regeneration were not investigated.

6.4. Gamma-irradiation regeneration

Gamma-irradiation regeneration method involves the dispersion of the saturated composite in water via ultrasound sonication followed by exposing the composite to gamma source. Usually, ^{60}Co is used as the gamma-irradiation source at rate of 1 $kGy.H^{-1}$. The required irradiation does depend on the amount of the saturated adsorbent, which is determined by pre-experiments to ensure full degradation of the adsorbate. Lou et al. (2017) studied the regeneration of magnetized bentonite that used for methylene blue adsorption through gamma-irradiation. The study reported that the process of regeneration occurs in multi-steps. Firstly, exposing the solution to gamma irradiation produces radiolytic products •OH and e^-_{eq}. Secondly; the electrons are trapped at the adsorbent surface and react with adsorbed molecular O_2 to form superoxide anion radical $\bullet O_2$. Both •OH and $\bullet O_2$ are strong oxidizing species that can decompose methylene blue adsorbed on the composite surface. The magnetized bentonite attained nine regeneration cycles with a slight decrease in the adsorption capacity from 75 mg/g to 60 mg/g. The reactions are shown below.

$$H_2O \xrightarrow{gamma\ irradiation} e^-_{qe} + H^+_2O \quad (1)$$

$$H^+_2O \rightarrow \bullet OH + H^+ \quad (2)$$

$$e^-_{qe} + O_2 \rightarrow \bullet O^-_2 \quad (3)$$

Similarly, a study showed that Fe_3O_4/Bentonite composite used for methylene blue removal was regenerated through gamma irradiation (Lou et al., 2015a). The study showed that the composite adsorption capacity remained constant over the entire 10 cycles. Thus, gamma irradiation is very effective in clay minerals composites regeneration as it can achieve complete degradation of the organic pollutant adsorbed by the adsorbent and retain constant adsorption capacity through several cycles. However, the effect of gamma-irradiation on the adsorbent physicochemical properties, morphology as well as structure was not addressed. Fig. 5 summarizes the re-generation methods performance for clay minerals composites regeneration. Whilst Fig. 6 illustrates the performance of regenerated adsorbents for methylene blue removal through several cycles.

7. Summary and future perspective

This review highlighted the performance of clay/minerals composites for the removal of organic water pollutants, focusing on the enhancement in their physiochemical and structure characteristics compared to their individual components. Also, the paper discussed the uptake mechanism of various clay/minerals composites and their performance after several regeneration cycles.

The literature showed that clay/minerals composites have great potential in organic pollutants removal from wastewater, which can lead to considerable innovations in wastewater treatment processes. Clay/minerals composites showed an increase in the adsorption capacity towards organic water pollutants compared to those raw and modified. The key elements responsible for such enhancement are the surface functional groups and the increase in the swelling ability. The reduction in specific surface area of the composite compared to its individual components does not necessarily imply that the adsorption capacity is reduced. Besides adsorption, clay/minerals composites have a degradation capability, which is mostly a property for clay mineral/metal oxides composites. In addition, the intercalating of other material into clay/minerals matrix influence the basal spacing, pore volume, hydrophobicity and swelling behavior, which affects the composite adsorption capacity. It is worth noting that the solution pH affects the swelling ability, and the uptake mechanism, especially when the electrostatic interaction is the main adsorption mechanism. The water matrices influence the composite uptake efficiency. From the above-mentioned studies, it was noticed that the adsorption is highest in distilled water > tap water > groundwater > industrial wastewater> sea water. The ionic strength may decrease or increase the adsorption depending on the uptake mechanism, but in some cases, the interfering ions do not influence the adsorption process due to the reactivity of these ions with the aqueous solution. Furthermore, clay/minerals composites attained higher thermal and mechanical stability, especially for clay/minerals-chitosan composites, which enhances their performance during the adsorption process. Desorption and regeneration studies indicated that clay/minerals composites could be utilized up to 10 regeneration cycles. Among the used regeneration methods, a constant adsorption capacity over several cycles could be achieved through gamma-irradiation regeneration technique. However, the high cost of gamma-irradiation technique limits its application. It is worth mentioning that the use of

water as an eluent in the chemical regeneration process is not efficient in case the adsorption is a chemisorption process.

The literature research showed a lack of studies related to kaolinite/polymeric, kaolinite /chitosan and kaolinite/carbonaceous composites for organic water pollutants removal. An interesting area of research is the synthesis of clay minerals composites or modification of clay/minerals using microwave assisted procedures. Also, the effect of microwave parameters on the clay/minerals morphology and physiochemical properties should be investigated. In addition, the majority of the adsorption studies focused on dye effluents. Therefore, a great deal of work is still needed to predict the performance of clay/minerals composites towards phenolic, antibiotics, herbicides, pesticides, oil, and real wastewater, besides their performance in a multipollutant system. In addition to adsorption, clay minerals composites showed a decent photocatalytic degradation capability. This implies that investigations on clay mineral composites degradation capability is needed. Besides, more work is needed to explore the capability of clay/minerals composites in other applications such as incorporating them into membrane matrix to enhance the membrane physiochemical properties and contribute to the treatment process by adsorption. Also, few studies showed that clay mineral composites attain good antibacterial activity, but more work should be done to draw a conclusion about their antibacterial activity. In addition, most of the studies are lab-scale. Therefore, the feasibility of clay/minerals composites on commercial scale should be investigated. More work is needed to increase the selectivity of clay/minerals composites towards specific organic pollutant. Currently, most of the studies focus on increasing the adsorption capacity without considering the selectivity. In our opinion, considering the adsorption capacity and performance after regeneration, clay/minerals-carbonaceous composite seems promising and worth further research to enhance their selectivity, economic viability, and performance on the commercial scale. In addition, the regeneration of clay/minerals composites was mainly implemented through chemical regeneration followed by gamma-irradiation, ultrasonic and thermal regeneration. However, the effect of the regeneration method on the composite morphology, structure and physiochemical properties was not investigated. Hence, future research should address the changes imposed by the regeneration method and consider evaluating other more modern regeneration techniques, such as electrochemical oxidation, microwave and photo-Fenton methods. Finally, it is important to combine the data of the composite characterization, adsorption experiments and molecular simulation to have better insights into the clay/minerals composites adsorption mechanism. The density functional theory (DFT) is a strong technique that can help in understanding the adsorption mechanism. The available research results hold significant promise for the use of clay minerals composites for organic water pollutants removal, especially bentonite/carbonaceous composites due to their high stability, adsorption capacity and regeneration capability.

Declaration of Competing Interest

The authors declare that they have no known competing financial interests or personal relationships that could have appeared to influence the work reported in this paper.

Data availability

No data was used for the research described in the article.

Acknowledgments

This publication was made possible by an Award [GSRA6-2-0516-19029] from Qatar National Research Fund (a member of Qatar Foundation). The contents herein are solely the responsibility of the author [s]. Open access funding is provided by the Qatar National Library.

References

Abukhadra, M.R., Adlii, A., Bakry, B.M., 2019a. Green fabrication of bentonite/chitosan@cobalt oxide composite (BE/CH@Co) of enhanced adsorption and advanced oxidation removal of Congo red dye and Cr (VI) from water. Int. J. Biol. Macromol. 126, 402–413.

Abukhadra, M.R., Refay, N.M., El-Sherbeeny, A.M., Mostafa, A.M., Elmeligy, M.A., 2019b. Facile synthesis of bentonite/biopolymer composites as low-cost carriers for 5-fluorouracil drug; equilibrium studies and pharmacokinetic behavior. Int. J. Biol. Macromol. 141, 721–731.

Acosta-Ferreira, S., Castillo, O.S., Madera-Santana, J.T., Mendoza-García, D.A., Núñez-Colín, C.A., Grijalva-Verdugo, C., Villa-Lerma, A.G., Morales-Vargas, A.T., Rodríguez-Núñez, J.R., 2020. Production and physicochemical characterization of chitosan for the harvesting of wild microalgae consortia. Biotechnol. Rep. 28, e00554.

Ahmad, R., Ansari, K., 2021. Comparative study for adsorption of Congo red and methylene blue dye on chitosan modified hybrid nanocomposite. Process Biochem. 108, 90–102.

Ahmad, R., Mirza, A., 2018. Synthesis of Guar gum/bentonite a novel bionanocomposite: Isotherms, kinetics and thermodynamic studies for the removal of Pb (II) and crystal violet dye. J. Mol. Liq. 249, 805–814.

Ain, Q.U., Rasheed, U., Yaseen, M., Zhang, H., He, R., Tong, Z., 2020a. Fabrication of magnetically separable 3-acrylamidopropyltrimethylammonium chloride intercalated bentonite composite for the efficient adsorption of cationic and anionic dyes. Appl. Surf. Sci. 514, 145929.

Ain, Q.U., Rasheed, U., Yaseen, M., Zhang, H., Tong, Z., 2020b. Superior dye degradation and adsorption capability of polydopamine modified Fe3O4-pillared bentonite composite. J. Hazard. Mater. 397, 122758.

Albatrni, H., Qiblawey, H., Almomani, F., Adham, S., Khraisheh, M., 2019. Polymeric adsorbents for oil removal from water. Chemosphere 233, 809–817.

Almahri, A., 2022. The solid-state synthetic performance of bentonite stacked manganese ferrite nanoparticles: adsorption and photo-Fenton degradation of MB dye and antibacterial applications. J. Mater. Res. Technol. 17, 2935–2949.

Almeida, C.A.P., Debacher, N.A., Downs, A.J., Cottet, L., Mello, C.A.D., 2009. Removal of methylene blue from colored effluents by adsorption on montmorillonite clay. J. Colloid Interface Sci. 332, 46–53.

Anirudhan, T.S., Tharun, A.R., 2012. Preparation and adsorption properties of a novel interpenetrating polymer network (IPN) containing carboxyl groups for basic dye from aqueous media. Chem. Eng. J. 181-182, 761–769.

Ansari, R., Sadati, S.M., Mozafari, N., Ashrafi, H., Azadi, A., 2020. Carbohydrate polymer-based nanoparticle application in drug delivery for CNS-related disorders. Eur. Polym. J. 128, 109607.

Arabkhani, P., Asfaram, A., Ateia, M., 2020. Easy-to-prepare graphene oxide/sodium montmorillonite polymer nanocomposite with enhanced adsorption performance. J. Water Process Eng. 38, 101651.

Arif, M., Liu, G., Yousaf, B., Ahmed, R., Irshad, S., Ashraf, A., Zia-ur-Rehman, M., Rashid, M.S., 2021. Synthesis, characteristics and mechanistic insight into the clays and clay minerals-biochar surface interactions for contaminants removal-a review. J. Clean. Prod. 310, 127548.

Ashiq, A., Adassooriya, N.M., Sarkar, B., Rajapaksha, A.U., Ok, Y.S., Vithanage, M., 2019. Municipal solid waste biochar-bentonite composite for the removal of antibiotic ciprofloxacin from aqueous media. J. Environ. Manag. 236, 428–435.

Askalany, A., Ali, E.S., Mohammed, R.H., 2020. A novel cycle for adsorption desalination system with two stages-ejector for higher water production and efficiency. Desalination 496, 114753.

Awad, A.M., Shaikh, S.M.R., Jalab, R., Gulied, M.H., Nasser, M.S., Benamor, A., Adham, S., 2019. Adsorption of organic pollutants by natural and modified clays: a comprehensive review. Sep. Purif. Technol. 228, 115719.

Azha, S.F., Shahadat, M., Ismail, S., 2017. Acrylic polymer emulsion supported bentonite clay coating for the analysis of industrial dye. Dyes Pigments 145, 550–560.

Barreca, S., Orecchio, S., Pace, A., 2014. The effect of montmorillonite clay in alginate gel beads for polychlorinated biphenyl adsorption: Isothermal and kinetic studies. Appl. Clay Sci. 99, 220–228.

Bermúdez, Y.H., Truffault, L., Pulcinelli, S.H., Santilli, C.V., 2018. Sodium montmorillonite/ureasil-poly(oxyethylene) nanocomposite as potential adsorbent of cationic dye. Appl. Clay Sci. 152, 158–165.

Bhattacharjee, C., Dutta, S., Saxena, V.K., 2020. A review on biosorptive removal of dyes and heavy metals from wastewater using watermelon rind as biosorbent. Environ. Adv. 2, 100007.

Bullock, A., 2006. Water – A Shared Responsibility: The United Nations World Water Development Report 2.

Cao, Y., Zhou, G., Zhou, R., Wang, C., Chi, B., Wang, Y., Hua, C., Qiu, J., Jin, Y., Wu, S., 2020. Green synthesis of reusable multifunctional γ-Fe2O3/bentonite modified by doped TiO2 hollow spherical nanocomposite for removal of BPA. Sci. Total Environ. 708, 134669.

Chang, J., Ma, J., Ma, Q., Zhang, D., Qiao, N., Hu, M., Ma, H., 2016. Adsorption of methylene blue onto Fe3O4/activated montmorillonite nanocomposite. Appl. Clay Sci. 119, 132–140.

Chauhan, M., Saini, V.K., Suthar, S., 2020. Ti-pillared montmorillonite clay for adsorptive removal of amoxicillin, imipramine, diclofenac-sodium, and paracetamol from water. J. Hazard. Mater. 399, 122832.

Chen, L., Zhou, C.H., Fiore, S., Tong, D.S., Zhang, H., Li, C.S., Ji, S.F., Yu, W.H., 2016. Functional magnetic nanoparticle/clay mineral nanocomposites: preparation, magnetism and versatile applications. Appl. Clay Sci. 127-128, 143–163.

Chen, Z., Wang, T., Jin, X., Chen, Z., Megharaj, M., Naidu, R., 2013. Multifunctional kaolinite-supported nanoscale zero-valent iron used for the adsorption and degradation of crystal violet in aqueous solution. J. Colloid Interface Sci. 398, 59–66.
Cheng, K., Heidari, Z., 2018. A new method for quantifying cation exchange capacity in clay minerals. Appl. Clay Sci. 161, 444–455.
Chua, S.F., Nouri, A., Ang, W.L., Mahmoudi, E., Mohammad, A.W., Benamor, A., Ba-Abbad, M., 2021. The emergence of multifunctional adsorbents and their role in environmental remediation. J. Environ. Chem. Eng. 9, 104793.
Combatt, M.P.M., Amorim, W.C.S., Brito, E.M.d.S., Cupertino, A.F., Mendonça, R.C.S., Pereira, H.A., 2020. Design of parallel plate electrocoagulation reactors supplied by photovoltaic system applied to water treatment. Comput. Electron. Agric. 177, 105676.
Cottet, L., Almeida, C.A.P., Naidek, N., Viante, M.F., Lopes, M.C., Debacher, N.A., 2014. Adsorption characteristics of montmorillonite clay modified with iron oxide with respect to methylene blue in aqueous media. Appl. Clay Sci. 95, 25–31.
Dai, H., Huang, Y., Huang, H., 2018. Eco-friendly polyvinyl alcohol/carboxymethyl cellulose hydrogels reinforced with graphene oxide and bentonite for enhanced adsorption of methylene blue. Carbohydr. Polym. 185, 1–11.
Dai, W.-J., Wu, P., Liu, D., Hu, J., Cao, Y., Liu, T.-Z., Okoli, C.P., Wang, B., Li, L., 2020. Adsorption of Polycyclic Aromatic Hydrocarbons from aqueous solution by Organic Montmorillonite Sodium Alginate Nanocomposites. Chemosphere 251, 126074.
Daraee, M., Saeedirad, R., Rashidi, A., 2019. Adsorption of hydrogen sulfide over a novel metal organic framework –metal oxide nanocomposite: TOUO-x (TiO2/UiO-66). J. Solid State Chem. 278, 120866.
Dehghani, M.H., Zarei, A., Mesdaghinia, A., Nabizadeh, R., Alimohammadi, M., Afsharnia, M., McKay, G., 2018. Production and application of a treated bentonite–chitosan composite for the efficient removal of humic acid from aqueous solution. Chem. Eng. Res. Des. 140, 102–115.
Diagboya, P.N., Olu-Owolabi, B.I., Mtunzi, F.M., Adebowale, K.O., 2020. Clay-carbonaceous material composites: Towards a new class of functional adsorbents for water treatment. Surf. Interfaces 19, 100506.
Dietel, J., Ufer, K., Kaufhold, S., Dohrmann, R., 2019. Crystal structure model development for soil clay minerals – II. Quantification and characterization of hydroxy-interlayered smectite (HIS) using the Rietveld refinement technique. Geoderma 347, 1–12.
Dotto, G.L., Rodrigues, F.K., Tanabe, E.H., Fröhlich, R., Bertuol, D.A., Martins, T.R., Foletto, E.L., 2016. Development of chitosan/bentonite hybrid composite to remove hazardous anionic and cationic dyes from colored effluents. J. Environ. Chem. Eng. 4, 3230–3239.
Duan, C., Ma, T., Wang, J., Zhou, Y., 2020. Removal of heavy metals from aqueous solution using carbon-based adsorbents: a review. J. Water Process Eng. 37, 101339.
Duman, O., Tunç, S., 2009. Electrokinetic and rheological properties of Na-bentonite in some electrolyte solutions. Microporous Mesoporous Mater. 117, 331–338.
Duman, O., Tunç, S., Bozoğlan, B.K., Polat, T.G., 2016a. Removal of triphenylmethane and reactive azo dyes from aqueous solution by magnetic carbon nanotube-κ-carrageenan-Fe3O4 nanocomposite. J. Alloys Compd. 687, 370–383.
Duman, O., Tunç, S., Polat, T.G., Bozoğlan, B.K., 2016b. Synthesis of magnetic oxidized multiwalled carbon nanotube-κ-carrageenan-Fe3O4 nanocomposite adsorbent and its application in cationic Methylene Blue dye adsorption. Carbohydr. Polym. 147, 79–88.
Duman, O., Özcan, C., Gürkan Polat, T., Tunç, S., 2019. Carbon nanotube-based magnetic and non-magnetic adsorbents for the high-efficiency removal of diquat dibromide herbicide from water: OMWCNT, OMWCNT-Fe(3)O(4) and OMWCNT-κ-carrageenan-Fe(3)O(4) nanocomposites. Environ. Pollut. (Barking, Essex: 1987) 244, 723–732.
E, T., Ma, D., Yang, S., Hao, X., 2020. Graphene oxide-montmorillonite/sodium alginate aerogel beads for selective adsorption of methylene blue in wastewater. J. Alloys Compd. 832, 154833.
El-Dib, F.I., Tawfik, F.M., Eshaq, G., Hefni, H.H.H., ElMetwally, A.E., 2016. Remediation of distilleries wastewater using chitosan immobilized Bentonite and Bentonite based organoclays. Int. J. Biol. Macromol. 86, 750–755.
El-Kousy, S.M., El-Shorbagy, H.G., El-Ghaffar, M.A.A., 2020. Chitosan/montmorillonite composites for fast removal of methylene blue from aqueous solutions. Mater. Chem. Phys. 254, 123236.
Elsherbiny, A.S., El-Hefnawy, M.E., Gemeay, A.H., 2017. Linker impact on the adsorption capacity of polyaspartate/montmorillonite composites towards methyl blue removal. Chem. Eng. J. 315, 142–151.
Ewis, D., Hameed, B.H., 2021. A review on microwave-assisted synthesis of adsorbents and its application in the removal of water pollutants. J. Water Process Eng. 41, 102006.
Ewis, D., Benamor, A., Ba-Abbad, M.M., Nasser, M., El-Naas, M., Qiblawey, H., 2020. Removal of Oil Content from Oil-Water Emulsions using Iron Oxide/Bentonite Nano Adsorbents. J. Water Process Eng. 38, 101583.
Ewis, D., Ismail, N.A., Hafiz, M., Benamor, A., Hawari, A.H., 2021. Nanoparticles functionalized ceramic membranes: fabrication, surface modification, and performance. Environ. Sci. Pollut. Res. 28, 12256–12281.
Ewis, D., Ba-Abbad, M.M., Benamor, A., Mahmud, N., Nasser, M., El-Naas, M., Mohammad, A.W., 2022a. Adsorption of 4-Nitrophenol onto Iron Oxide Bentonite Nanocomposite: Process Optimization, Kinetics, Isotherms and Mechanism. Int. J. Environ. Res. 16, 23.
Ewis, D., Mahmud, N., Benamor, A., Ba-Abbad, M.M., Nasser, M., El-Naas, M., 2022b. Enhanced Removal of Diesel Oil using New magnetic Bentonite-based Adsorbents combined with Different Carbon sources. Water Air Soil Pollut. 233, 195.
Fabryanty, R., Valencia, C., Edi-Soetaredjo, F., Putro, J., Santoso, S., Kurniawan, A., Ju, Y.-H., Ismadji, S., 2017. Removal of crystal violet dye by adsorption using Bentonite – Alginate Composite. J. Environ. Chem. Eng. 5.
Fei, F., Gao, Z., Wu, H., Wurendaodi, W., Zhao, S., Asuha, S., 2020. Facile solid-state synthesis of Fe3O4/kaolinite nanocomposites for enhanced dye adsorption. J. Solid State Chem. 291, 121655.
Ferreira, B.F., Ciuffi, K.J., Nassar, E.J., Vicente, M.A., Trujillano, R., Rives, V., de Faria, E. H., 2017. Kaolinite-polymer compounds by grafting of 2-hydroxyethyl methacrylate and 3-(trimethoxysilyl)propyl methacrylate. Appl. Clay Sci. 146, 526–534.
Fil, B.A., 2016. Isotherm, kinetic, and thermodynamic studies on the adsorption behavior of malachite green dye onto montmorillonite clay. Part. Sci. Technol. 34, 118–126.
Foroutan, R., Mohammadi, R., MousaKhanloo, F., Sahebi, S., Ramavandi, B., Kumar, P.S., Vardhan, K.H., 2020. Performance of montmorillonite/graphene oxide/CoFe2O4 as a magnetic and recyclable nanocomposite for cleaning methyl violet dye-laden wastewater. Adv. Powder Technol. 31, 3993–4004.
Garmia, D., Zaghouane-Boudiaf, H., Ibbora, C.V., 2018. Preparation and characterization of new low cost adsorbent beads based on activated bentonite encapsulated with calcium alginate for removal of 2,4-dichlorophenol from aqueous medium. Int. J. Biol. Macromol. 115, 257–265.
Ge, Y., Cui, X., Liao, C., Li, Z., 2017. Facile fabrication of green geopolymer/alginate hybrid spheres for efficient removal of Cu(II) in water: batch and column studies. Chem. Eng. J. 311, 126–134.
Gkika, D.A., Liakos, E.V., Vordos, N., Kontogoulidou, C., Magafas, L., Bikiaris, D.N., Bandekas, D.V., Mitropoulos, A.C., Kyzas, G.Z., 2019. Cost Estimation of Polymeric Adsorbents. Polymers 11.
Gopal, G., Kvg, R., Mj, S., J, L.A.A., Chandrasekaran, N., Mukherjee, A., 2020. Green synthesized Fe/Pd and in-situ Bentonite-Fe/Pd composite for efficient tetracycline removal. J. Environ. Chem. Eng. 8, 104126.
Guo, W., Hu, W., Pan, J., Zhou, H., Guan, W., Wang, X., Dai, J., Xu, L., 2011. Selective adsorption and separation of BPA from aqueous solution using novel molecularly imprinted polymers based on kaolinite/Fe3O4 composites. Chem. Eng. J. 171, 603–611.
Gusain, R., Kumar, N., Ray, S.S., 2020. Recent advances in carbon nanomaterial-based adsorbents for water purification. Coord. Chem. Rev. 405, 213111.
Guz, L., Curutchet, G., Torres Sánchez, R.M., Candal, R., 2014. Adsorption of crystal violet on montmorillonite (or iron modified montmorillonite) followed by degradation through Fenton or photo-Fenton type reactions. J. Environ. Chem. Eng. 2, 2344–2351.
He, X., Male, K.B., Nesterenko, P.N., Brabazon, D., Paull, B., Luong, J.H.T., 2013. Adsorption and Desorption of Methylene Blue on Porous Carbon Monoliths and Nanocrystalline Cellulose. ACS Appl. Mater. Interfaces 5, 8796–8804.
Hizal, J., Apak, R., 2006. Modeling of copper(II) and lead(II) adsorption on kaolinite-based clay minerals individually and in the presence of humic acid. J. Colloid Interface Sci. 295, 1–13.
Hojiyev, R., Ulcay, Y., Celik, M., 2017. Development of a clay-polymer compatibility approach for nanocomposite applications. Appl. Clay Sci. 146, 548–556.
Huang, R., Zhang, L., Hu, P., Wang, J., 2016. Adsorptive removal of Congo red from aqueous solutions using crosslinked chitosan and crosslinked chitosan immobilized bentonite. Int. J. Biol. Macromol. 86, 496–504.
Ifthikar, J., Jiao, X., Ngambia, A., Wang, T., Khan, A., Jawad, A., Xue, Q., Liu, L., Chen, Z., 2018. Facile One-Pot Synthesis of Sustainable Carboxymethyl Chitosan – Sewage Sludge Biochar for Effective Heavy Metal Chelation and Regeneration. Bioresour. Technol. 262, 22–31.
Ihsanullah, I., Jamal, A., Ilyas, M., Zubair, M., Khan, G., Atieh, M.A., 2020. Bioremediation of dyes: current status and prospects. J. Water Process Eng. 38, 101680.
Jana, S., Ray, J., Mondal, B., Tripathy, T., 2019. Efficient and selective removal of cationic organic dyes from their aqueous solutions by a nanocomposite hydrogel, katira gum-cl-poly(acrylic acid-co-N, N-dimethylacrylamide)@bentonite. Appl. Clay Sci. 173, 46–64.
Jawad, A.H., Mohammed, I.A., Abdulhameed, A.S., 2020. Tuning of Fly Ash Loading into Chitosan-Ethylene Glycol Diglycidyl Ether Composite for Enhanced Removal of Reactive Red 120 Dye: Optimization Using the Box–Behnken Design. J. Polym. Environ. 28, 2720–2733.
Jun, B.-M., Al-Hamadani, Y.A.J., Son, A., Park, C.M., Jang, M., Jang, A., Kim, N.C., Yoon, Y., 2020. Applications of metal-organic framework based membranes in water purification: a review. Sep. Purif. Technol. 247, 116947.
Khan, T.A., Khan, E.A., Shahjahan, 2015. Removal of basic dyes from aqueous solution by adsorption onto binary iron-manganese oxide coated kaolinite: Non-linear isotherm and kinetics modeling. Appl. Clay Sci. 107, 70–77.
Khanlari, S., Dubé, M., 2015. Effect of pH on Poly(acrylic acid) solution Polymerization. J. Macromol. Sci. 52.
Khatamian, M., Divband, B., Shahi, R., 2019. Ultrasound assisted co-precipitation synthesis of Fe3O4/ bentonite nanocomposite: Performance for nitrate, BOD and COD water treatment. J. Water Process Eng. 31, 100870.
Khodabakhshloo, N., Biswas, B., Moore, F., Du, J., Naidu, R., 2021. Organically functionalized bentonite for the removal of perfluorooctane sulfonate, phenanthrene and copper mixtures from wastewater. Appl. Clay Sci. 200, 105883.
Kilduff, J.E., King, C.J., 1997. Effect of Carbon Adsorbent Surface Properties on the Uptake and Solvent Regeneration of Phenol. Ind. Eng. Chem. Res. 36, 1603–1613.
Kittinaovarat, S., Kansomwan, P., Jiratumnukul, N., 2010. Chitosan/modified montmorillonite beads and adsorption Reactive Red 120. Appl. Clay Sci. 48, 87–91.
Kong, L., Tian, Y., Li, N., Liu, Y., Zhang, J., Zhang, J., Zuo, W., 2018. Highly-effective phosphate removal from aqueous solutions by calcined nano-porous palygorskite matrix with embedded lanthanum hydroxide. Appl. Clay Sci. 162, 507–517.
Kong, Y., Wang, L., Ge, Y., Su, H., Li, Z., 2019. Lignin xanthate resin–bentonite clay composite as a highly effective and low-cost adsorbent for the removal of doxycycline hydrochloride antibiotic and mercury ions in water. J. Hazard. Mater. 368, 33–41.

Lauriches se, S., Avérous, L., 2014. Chemical modification of lignins: Towards biobased polymers. Prog. Polym. Sci. 39, 1266–1290.
Lazaratou, C.V., Vayenas, D.V., Papoulis, D., 2020. The role of clays, clay minerals and clay-based materials for nitrate removal from water systems: a review. Appl. Clay Sci. 185, 105377.
Li, H., Song, S., Dong, X., Min, F., Zhao, Y., Peng, C., Nahmad, Y., 2018. Molecular Dynamics Study of Crystalline Swelling of Montmorillonite as Affected by Interlayer Cation Hydration. JOM 70, 479–484.
Li, J., Cai, J., Zhong, L., Cheng, H., Wang, H., Ma, Q., 2019. Adsorption of reactive red 136 onto chitosan/montmorillonite intercalated composite from aqueous solution. Appl. Clay Sci. 167, 9–22.
Li, Q., Yue, Q.-Y., Sun, H.-J., Su, Y., Gao, B.-Y., 2010. A comparative study on the properties, mechanisms and process designs for the adsorption of non-ionic or anionic dyes onto cationic-polymer/bentonite. J. Environ. Manag. 91, 1601–1611.
Li, Q., Su, Y., Yue, Q.-Y., Gao, B.-Y., 2011. Adsorption of acid dyes onto bentonite modified with polycations: Kinetics study and process design to minimize the contact time. Appl. Clay Sci. 53, 760–765.
Li, W., Kan, X., Zeng, T., Li, S., Cheng, R., Zhou, M., Hou, H., 2022. MoS2/Bentonite prepared by a facile method for efficient removal of Cd2+ from aqueous solution. J. Alloys Compd. 907, 164508.
Liang, X., Lu, Y., Li, Z., Yang, C., Niu, C., Su, X., 2017. Bentonite/carbon composite as highly recyclable adsorbents for alkaline wastewater treatment and organic dye removal. Microporous Mesoporous Mater. 241, 107–114.
Lin, D., Zhao, Q., Hu, L., Xing, B., 2014. Synthesis and characterization of cubic mesoporous bridged polysilsesquioxane for removing organic pollutants from water. Chemosphere 103, 188–196.
Liu, A., Zhou, W., Shen, K., Liu, J., Zhang, X., 2015a. One-pot hydrothermal synthesis of hematite-reduced graphene oxide composites for efficient removal of malachite green from aqueous solution. RSC Adv. 5, 17336–17342.
Liu, J., Shi, S., Li, C., Hong, X., Gu, Z., Li, F., Zhai, J., Zhang, Q., Liao, J., Liu, N., Liu, C., 2021. U(VI) adsorption by one-step hydrothermally synthesized cetyltrimethylammonium bromide modified hydroxyapatite-bentonite composites from phosphate-carbonate coexisted solution. Appl. Clay Sci. 203, 106027.
Liu, Q., Yang, B., Zhang, L., Huang, R., 2015b. Adsorption of an anionic azo dye by cross-linked chitosan/bentonite composite. Int. J. Biol. Macromol. 72, 1129–1135.
Liu, S., Liu, Y., Jiang, L., Zeng, G., Li, Y., Zeng, Z., Wang, X., Ning, Q., 2019a. Removal of 17β-Estradiol from water by adsorption onto montmorillonite-carbon hybrids derived from pyrolysis carbonization of carboxymethyl cellulose. J. Environ. Manag. 236, 25–33.
Liu, S., Liu, Y., Jiang, L., Zeng, G., Li, Y., Zeng, Z., Wang, X., Ning, Q., 2019b. Removal of 17β-Estradiol from water by adsorption onto montmorillonite-carbon hybrids derived from pyrolysis carbonization of carboxymethyl cellulose. J. Environ. Manag. 236, 25–33.
Liu, Y.N., Dong, C., Wei, H., Yuan, W., Li, K., 2015. Adsorption of levofloxacin onto an iron-pillared montmorillonite (clay mineral): Kinetics, equilibrium and mechanism. Appl. Clay Sci. 118, 301–307.
Lou, Z., Zhou, Z., Zhang, W., Zhang, X., Hu, X., Liu, P., Zhang, H., 2015a. Magnetized bentonite by Fe3O4 nanoparticles treated as adsorbent for methylene blue removal from aqueous solution: Synthesis, characterization, mechanism, kinetics and regeneration. J. Taiwan Inst. Chem. Eng. 49, 199–205.
Lou, Z., Zhou, Z., Zhang, W., Zhang, X., Hu, X., Liu, P., Zhang, H., 2015b. Magnetized bentonite by Fe3O4 nanoparticles treated as adsorbent for methylene blue removal from aqueous solution: Synthesis, characterization, mechanism, kinetics and regeneration. J. Taiwan Inst. Chem. Eng. 49, 199–205.
Lou, Z., Zhang, W., Hu, X., Zhang, H., 2017. Synthesis of a novel functional group-bridged magnetized bentonite adsorbent: Characterization, kinetics, isotherm, thermodynamics and regeneration. Chin. J. Chem. Eng. 25, 587–594.
Mahdavinia, G., Baghban, A., Zorofi, S., Massoudi, A., 2014. Kappa-Carrageenan biopolymer-based nanocomposite hydrogel and adsorption of methylene blue cationic dye from water. J. Mater. Environ. Sci. 5, 330–337.
Mahmoud, M.E., El-Ghanam, A.M., Mohamed, R.H.A., Saad, S.R., 2020. Enhanced adsorption of Levofloxacin and Ceftriaxone antibiotics from water by assembled composite of nanotitanium oxide/chitosan/nano-bentonite. Mater. Sci. Eng. C Mater. Biol. Appl. 108, 110199.
Mansour, F., Al-Hindi, M., Yahfoufi, R., Ayoub, G.M., Ahmad, M.N., 2018. The use of activated carbon for the removal of pharmaceuticals from aqueous solutions: a review. Rev. Environ. Sci. Biotechnol. 17, 109–145.
Marrakchi, F., Hameed, B.H., Hummadi, E.H., 2020. Mesoporous biohybrid epichlorohydrin crosslinked chitosan/carbon–clay adsorbent for effective cationic and anionic dyes adsorption. Int. J. Biol. Macromol. 163, 1079–1086.
Md. Munjur, H., Hasan, M.N., Awual, M.R., Islam, M.M., Shenashen, M.A., Iqbal, J., 2020. Biodegradable natural carbohydrate polymeric sustainable adsorbents for efficient toxic dye removal from wastewater. J. Mol. Liq. 319, 114356.
Minisy, I.M., Salahuddin, N.A., Ayad, M.M., 2021a. Adsorption of methylene blue onto chitosan–montmorillonite/polyaniline nanocomposite. Appl. Clay Sci. 203, 105993.
Minisy, I.M., Salahuddin, N.A., Ayad, M.M., 2021b. Adsorption of methylene blue onto chitosan–montmorillonite/polyaniline nanocomposite. Appl. Clay Sci. 203, 105993.
Momina, Mohammad S., Suzylawati, I., 2020. Study of the adsorption/desorption of MB dye solution using bentonite adsorbent coating. J. Water Process Eng. 34, 101155.
Morais da Silva, P.M., Camparotto, N.G., Grego Lira, K.T., Franco Picone, C.S., Prediger, P., 2020. Adsorptive removal of basic dye onto sustainable chitosan beads: Equilibrium, kinetics, stability, continuous-mode adsorption and mechanism. Sustain. Chem. Pharm. 18, 100318.
Muhammad, Y., Rashid, H.U., Subhan, S., Rahman, A.U., Sahibzada, M., Tong, Z., 2019. Boosting the hydrodesulfurization of dibenzothiophene efficiency of Mn decorated (Co/Ni)-Mo/Al2O3 catalysts at mild temperature and pressure by coupling with phosphonium based ionic liquids. Chem. Eng. J. 375, 121957.
Musarurwa, H., Tavengwa, N.T., 2020. Application of carboxymethyl polysaccharides as bio-sorbents for the sequestration of heavy metals in aquatic environments. Carbohydr. Polym. 237, 116142.
Najafi, H., Farajfaed, S., Zolgharnian, S., Mosavi Mirak, S.H., Asasian-Kolur, N., Sharifian, S., 2021. A comprehensive study on modified-pillared clays as an adsorbent in wastewater treatment processes. Process. Saf. Environ. Prot. 147, 8–36.
Neelaveni, M., Santhana Krishnan, P., Ramya, R., Sonia Theres, G., Shanthi, K., 2019. Montmorillonite/graphene oxide nanocomposite as superior adsorbent for the adsorption of Rhodamine B and Nickel ion in binary system. Adv. Powder Technol. 30, 596–609.
Ngoh, Y.S., Nawi, M.A., 2016. Fabrication and properties of an immobilized P25TiO2-montmorillonite bilayer system for the synergistic photocatalytic–adsorption removal of methylene blue. Mater. Res. Bull. 76, 8–21.
Ngulube, T., Gumbo, J.R., Masindi, V., Maity, A., 2017. An update on synthetic dyes adsorption onto clay based minerals: a state-of-art review. J. Environ. Manag. 191, 35–57.
Nigiz, F.U., 2019. Synthesis of a novel graphene–kaolin–alginate adsorbent for dye removal, and optimization of the adsorption by response surface methodology. Res. Chem. Intermed. 45, 3739–3753.
Olu-Owolabi, B.I., Alabi, A.H., Diagboya, P.N., Unuabonah, E.I., Düring, R.-A., 2017. Adsorptive removal of 2,4,6-trichlorophenol in aqueous solution using calcined kaolinite-biomass composites. J. Environ. Manag. 192, 94–99.
Olusegun, S.J., Mohallem, N.D.S., 2020. Comparative adsorption mechanism of doxycycline and Congo red using synthesized kaolinite supported CoFe2O4 nanoparticles. Environ. Pollut. 260, 114019.
Otunola, B.O., Ololade, O.O., 2020. A review on the application of clay minerals as heavy metal adsorbents for remediation purposes. Environ. Technol. Innov. 18, 100692.
Ouachtak, H., El Haouti, R., El Guerdaoui, A., Haounati, R., Amaterz, E., Addi, A.A., Akbal, F., Taha, M.L., 2020. Experimental and molecular dynamics simulation study on the adsorption of Rhodamine B dye on magnetic montmorillonite composite γ-Fe2O3@Mt. J. Mol. Liq. 309, 113142.
Oussalah, A., Boukerroui, A., Amina, A., Djellouli, B., 2018. Cationic and anionic dyes removal by low-cost hybrid alginate/natural bentonite composite beads: Adsorption and reusability studies. Int. J. Biol. Macromol. 124.
Oyewo, O.A., Elemike, E.E., Onwudiwe, D.C., Onyango, M.S., 2020. Metal oxide-cellulose nanocomposites for the removal of toxic metals and dyes from wastewater. Int. J. Biol. Macromol. 164, 2477–2496.
Ozbey-Unal, B., Omwene, P.I., Yagcioglu, M., Balcik-Canbolat, Ç., Karagunduz, A., Keskinler, B., Dizge, N., 2020. Treatment of organized industrial zone wastewater by microfiltration/reverse osmosis membrane process for water recovery: from lab to pilot scale. J. Water Process Eng. 38, 101646.
Peighambardoust, S.J., Aghamohammadi-Bavil, O., Foroutan, R., Arsalani, N., 2020. Removal of malachite green using carboxymethyl cellulose-g-polyacrylamide/montmorillonite nanocomposite hydrogel. Int. J. Biol. Macromol. 159, 1122–1131.
Peng, G., Li, T., Ai, B., Yang, S., Fu, J., He, Q., Yu, G., Deng, S., 2019. Highly efficient removal of enrofloxacin by magnetic montmorillonite via adsorption and persulfate oxidation. Chem. Eng. J. 360, 1119–1127.
Peng, X., Luan, Z., Zhang, H., 2006. Montmorillonite–Cu(II)/Fe(III) oxides magnetic material as adsorbent for removal of humic acid and its thermal regeneration. Chemosphere 63, 300–306.
Peternele, W.S., Monge Fuentes, V., Fascineli, M.L., Rodrigues da Silva, J., Silva, R.C., Lucci, C.M., Bentes de Azevedo, R., 2014. Experimental Investigation of the Coprecipitation Method: an Approach to Obtain Magnetite and Maghemite Nanoparticles with improved Properties. J. Nanomater. 2014, 682985.
Preetha, B.K., Vishalakshi, B., 2020. Microwave assisted synthesis of karaya gum based montmorillonite nanocomposite: Characterisation, swelling and dye adsorption studies. Int. J. Biol. Macromol. 154, 739–750.
Rahmani, H., Lakzian, A., Karimi, A., Halajnia, A., 2020a. Efficient removal of 2,4-dinitrophenol from synthetic wastewater and contaminated soil samples using free and immobilized laccases. J. Environ. Manag. 256, 109740.
Rahmani, S., Zeynizadeh, B., Karami, S., 2020b. Removal of cationic methylene blue dye using magnetic and anionic-cationic modified montmorillonite: kinetic, isotherm and thermodynamic studies. Appl. Clay Sci. 184, 105391.
Rihayat, T., Salim, S., Arlina, A., Fona, Z., Jalal, R., Alam, P.N., Zaimahwati, Sami M., Syarif, J., Juhan, N., 2018. Determination of CEC value (Cation Exchange Capacity) of Bentonites from North Aceh and Bener Meriah, Aceh Province, Indonesia using three methods. IOP Conf. Ser. Mater. Sci. Eng. 334, 012054.
Rotaru, A., Cojocaru, C., Cretescu, I., Pinteala, M., Timpu, D., Sacarescu, L., Harabagiu, V., 2014. Performances of clay aerogel polymer composites for oil spill sorption: Experimental design and modeling. Sep. Purif. Technol. 133, 260–275.
Sadiq, A.C., Rahim, N.Y., Suah, F.B.M., 2020. Adsorption and desorption of malachite green by using chitosan-deep eutectic solvents beads. Int. J. Biol. Macromol. 164, 3965–3973.
Sakin Omer, O., Hussein, M.A., Hussein, B.H.M., Mgaidi, A., 2018. Adsorption thermodynamics of cationic dyes (methylene blue and crystal violet) to a natural clay mineral from aqueous solution between 293.15 and 323.15 K. Arab. J. Chem. 11, 615–623.
Saleh, I.A., Zouari, N., Al-Ghouti, M.A., 2020. Removal of pesticides from water and wastewater: Chemical, physical and biological treatment approaches. Environ. Technol. Innov. 19, 101026.
Salvador, F., Martin-Sanchez, N., Sanchez-Hernandez, R., Sanchez-Montero, M.J., Izquierdo, C., 2015. Regeneration of carbonaceous adsorbents. Part II: Chemical, Microbiological and Vacuum Regeneration. Microporous Mesoporous Mater. 202, 277–296.

Sarkar, P., Dey, A., 2021. Phycoremediation – an emerging technique for dye abatement: an overview. Process. Saf. Environ. Prot. 147, 214–225.
Schell, W.R., Jordan, J.V., 1959. Anion-exchange studies of pure clays. Plant Soil 10, 303–318.
Şenol, Z.M., Çetinkaya, S., Yenidünya, A.F., Başoğlu-Ünal, F., Ece, A., 2022a. Epichlorohydrin and tripolyphosphate-crosslinked chitosan–kaolin composite for Auramine O dye removal from aqueous solutions: Experimental study and DFT calculations. Int. J. Biol. Macromol. 199, 318–330.
Şenol, Z.M., Çetinkaya, S., Yenidünya, A.F., Başoğlu-Ünal, F., Ece, A., 2022b. Epichlorohydrin and tripolyphosphate-crosslinked chitosan–kaolin composite for Auramine O dye removal from aqueous solutions: Experimental study and DFT calculations. Int. J. Biol. Macromol. 199, 318–330.
Shamsudin, M.S., Azha, S.F., Shahadat, M., Ismail, S., 2019. Cellulose/bentonite-zeolite composite adsorbent material coating for treatment of N-based antiseptic cationic dye from water. J. Water Process Eng. 29, 100764.
Shariatinia, Z., 2018. Carboxymethyl chitosan: Properties and biomedical applications. Int. J. Biol. Macromol. 120, 1406–1419.
Shen, T., Gao, M., 2019. Gemini surfactant modified organo-clays for removal of organic pollutants from water: a review. Chem. Eng. J. 375, 121910.
Sirajudheen, P., Karthikeyan, P., Basheer, M.C., Meenakshi, S., 2020. Adsorptive removal of anionic azo dyes from effluent water using Zr(IV) encapsulated carboxymethyl cellulose-montmorillonite composite. Environ. Chem. Ecotoxicol. 2, 73–82.
Tomul, F., Turgut Basoglu, F., Canbay, H., 2016. Determination of adsorptive and catalytic properties of copper, silver and iron contain titanium-pillared bentonite for the removal bisphenol a from aqueous solution. Appl. Surf. Sci. 360, 579–593.
Tong, D.S., Wu, C.W., Adebajo, M.O., Jin, G.C., Yu, W.H., Ji, S.F., Zhou, C.H., 2018. Adsorption of methylene blue from aqueous solution onto porous cellulose-derived carbon/montmorillonite nanocomposites. Appl. Clay Sci. 161, 256–264.
Uddin, M.K., 2017. A review on the adsorption of heavy metals by clay minerals, with special focus on the past decade. Chem. Eng. J. 308, 438–462.
Unuabonah, E.I., Taubert, A., 2014. Clay–polymer nanocomposites (CPNs): Adsorbents of the future for water treatment. Appl. Clay Sci. 99, 83–92.
Unuabonah, E.I., Adedapo, A.O., Nnamdi, C.O., Adewuyi, A., Omorogie, M.O., Adebowale, K.O., Olu-Owolabi, B.I., Ofomaja, A.E., Taubert, A., 2015. Successful scale-up performance of a novel papaya-clay combo adsorbent: up-flow adsorption of a basic dye. Desalin. Water Treat. 56, 536–551.
Upadhyay, U., Sreedhar, I., Singh, S.A., Patel, C.M., Anitha, K.L., 2021. Recent advances in heavy metal removal by chitosan based adsorbents. Carbohydr. Polym. 251, 117000.
Vakili, M., Deng, S., Cagnetta, G., Wang, W., Meng, P., Liu, D., Yu, G., 2019. Regeneration of chitosan-based adsorbents used in heavy metal adsorption: a review. Sep. Purif. Technol. 224, 373–387.
Vanamudan, A., Bandwala, K., Pamidimukkala, P., 2014. Adsorption property of Rhodamine 6G onto chitosan-g-(N-vinyl pyrrolidone)/montmorillonite composite. Int. J. Biol. Macromol. 69, 506–513.
Vårum, K.M., Ottøy, M.H., Smidsrød, O., 1994. Water-solubility of partially N-acetylated chitosans as a function of pH: effect of chemical composition and depolymerisation. Carbohydr. Polym. 25, 65–70.
Venancio, L.P.R., Silva, M.I.A., da Silva, T.L., Moschetta, V.A.G., de Campos Zuccari, D.A. P., Almeida, E.A., Bonini-Domingos, C.R., 2013. Pollution-induced metabolic responses in hypoxia-tolerant freshwater turtles. Ecotoxicol. Environ. Saf. 97, 1–9.
Vithalkar, S.H., Jugade, R.M., 2020. Adsorptive removal of crystal violet from aqueous solution by cross-linked chitosan coated bentonite. Mater. Today Proc. 29, 1025–1032.
Wan, D., Li, W., Wang, G., Chen, K., Lu, L., Hu, Q., 2015. Adsorption and heterogeneous degradation of rhodamine B on the surface of magnetic bentonite material. Appl. Surf. Sci. 349, 988–996.
Wang, B., Li, M., Zhang, H., Zhu, J., Chen, S., Ren, D., 2020a. Effect of straw-derived dissolved organic matter on the adsorption of sulfamethoxazole to purple paddy soils. Ecotoxicol. Environ. Saf. 203, 110990.
Wang, J., Tang, X., Xu, Y., Cheng, X., Li, G., Liang, H., 2020b. Hybrid UF/NF process treating secondary effluent of wastewater treatment plants for potable water reuse: Adsorption vs. coagulation for removal improvements and membrane fouling alleviation. Environ. Res. 188, 109833.
Wang, J., Wang, W., Ai, Z., Li, M., Li, H., Peng, W., Zhao, Y., Song, S., 2021. Adsorption toward Pb(II) occurring on three-dimensional reticular-structured montmorillonite hydrogel surface. Appl. Clay Sci. 210, 106153.
Wang, M.-m., Wang, L., 2013. Synthesis and characterization of carboxymethyl cellulose/organic montmorillonite nanocomposites and its adsorption behavior for Congo Red dye. Water Sci. Eng. 6, 272–282.
Wang, N., Xiao, F., Zhang, J., Zhou, H., Qin, Y., Pan, D., 2019. Spherical montmorillonite-supported nano-silver as a self-sedimentary catalyst for methylene blue removal. Appl. Clay Sci. 174, 146–151.
Wang, W., Wang, J., Zhao, Y., Bai, H., Huang, M., Zhang, T., Song, S., 2020c. High-performance two-dimensional montmorillonite supported-poly(acrylamide-co-acrylic acid) hydrogel for dye removal. Environ. Pollut. 257, 113574.
Wang, W., Fan, M., Ni, J., Peng, W., Cao, Y., Li, H., Huang, Y., Fan, G., Zhao, Y., Song, S., 2022. Efficient dye removal using fixed-bed process based on porous montmorillonite nanosheet/poly(acrylamide-co-acrylic acid)/sodium alginate hydrogel beads. Appl. Clay Sci. 219, 106443.
Wei, Y., Yuan, P., Liu, D., Losic, D., Tan, D., Chen, F., Liu, H., Zhou, J., Du, P., Song, Y., 2019. Activation of natural halloysite nanotubes by introducing lanthanum oxycarbonate nanoparticles via co-calcination for outstanding phosphate removal. Chem. Commun. 55, 2110–2113.
Wu, P., Zhou, J., Wang, X., Dai, Y., Dang, Z., Zhu, N., Li, P., Wu, J., 2011. Adsorption of Cu–EDTA complexes from aqueous solutions by polymeric Fe/Zr pillared montmorillonite: Behaviors and mechanisms. Desalination 277, 288–295.
Xie, L., Yang, D., Lu, Q., Zhang, H., Zeng, H., 2020. Role of molecular architecture in the modulation of hydrophobic interactions. Curr. Opin. Colloid Interface Sci. 47, 58–69.
Xiong, D.G., Zhang, Z., Huang, X.Y., Huang, Y., Yu, J., Cai, J.X., Yang, Z.Y., 2020. Boosting the polysulfide confinement in B/N–codoped hierarchically porous carbon nanosheets via Lewis acid–base interaction for stable Li–S batteries. J. Energy Chem. 51, 90–100.
Xu, W., Chen, Y., Zhang, W., Li, B., 2019. Fabrication of graphene oxide/bentonite composites with excellent adsorption performances for toluidine blue removal from aqueous solution. Adv. Powder Technol. 30, 493–501.
Yadav, V.B., Gadi, R., Kalra, S., 2019. Clay based nanocomposites for removal of heavy metals from water: a review. J. Environ. Manag. 232, 803–817.
Yang, W., Shi, X., Wang, J., Chen, W., Zhang, L., Zhang, W., Zhang, X., Lu, J., 2019a. Fabrication of a Novel Bifunctional Nanocomposite with improved Selectivity for Simultaneous Nitrate and Phosphate Removal from Water. ACS Appl. Mater. Interfaces 11, 35277–35285.
Yang, Y., Yu, W., He, S., Yu, S., Chen, Y., Lu, L., Shu, Z., Cui, H., Zhang, Y., Jin, H., 2019b. Rapid adsorption of cationic dye-methylene blue on the modified montmorillonite/graphene oxide composites. Appl. Clay Sci. 168, 304–311.
Yang, Y., Zhu, R., Chen, Q., Fu, H., He, Q., Zhu, J., He, H., 2020. A novel multifunctional adsorbent synthesized by modifying acidified organo-montmorillonite with iron hydroxides. Appl. Clay Sci. 185, 105420.
Yao, Y., Gao, B., Fang, J., Zhang, M., Chen, H., Zhou, Y., Creamer, A.E., Sun, Y., Yang, L., 2014. Characterization and environmental applications of clay–biochar composites. Chem. Eng. J. 242, 136–143.
Yildirim, A., Bulut, Y., 2020. Adsorption behaviors of malachite green by using crosslinked chitosan/polyacrylic acid/bentonite composites with different ratios. Environ. Technol. Innov. 17, 100560.
Yu, F., Bai, X., Liang, M., Ma, J., 2021. Recent progress on metal-organic framework-derived porous carbon and its composite for pollutant adsorption from liquid phase. Chem. Eng. J. 405, 126960.
Zeng, H., Singh, A., Basak, S., Ulrich, K.-U., Sahu, M., Biswas, P., Catalano, J.G., Giammar, D.E., 2009. Nanoscale size Effects on Uranium(VI) Adsorption to Hematite. Environ. Sci. Technol. 43, 1373–1378.
Zhang, C., Luan, J., Yu, X., Chen, W., 2019. Characterization and adsorption performance of graphene oxide – montmorillonite nanocomposite for the simultaneous removal of Pb2+ and p-nitrophenol. J. Hazard. Mater. 378, 120739.
Zhang, C., Zhang, S., Yang, Y., Yu, H., Dong, X., 2020a. Highly sensitive H2S sensors based on metal-organic framework driven γ-Fe2O3 on reduced graphene oxide composites at room temperature. Sensors Actuators B Chem. 325, 128804.
Zhang, H., Ma, J., Wang, F., Chu, Y., Yang, L., Xia, M., 2020b. Mechanism of carboxymethyl chitosan hybrid montmorillonite and adsorption of Pb(II) and Congo red by CMC-MMT organic-inorganic hybrid composite. Int. J. Biol. Macromol. 149, 1161–1169.
Zhang, L., Hu, P., Wang, J., Liu, Q., Huang, R., 2015. Adsorption of methyl orange (MO) by Zr (IV)-immobilized cross-linked chitosan/bentonite composite. Int. J. Biol. Macromol. 81, 818–827.
Zhang, L., Hu, P., Wang, J., Huang, R., 2016a. Adsorption of Amido black 10B from aqueous solutions onto Zr (IV) surface-immobilized cross-linked chitosan/bentonite composite. Appl. Surf. Sci. 369, 558–566.
Zhang, L., Zeng, Y., Cheng, Z., 2016b. Removal of heavy metal ions using chitosan and modified chitosan: a review. J. Mol. Liq. 214, 175–191.
Zhang, Q., Xu, L., 2012. Simulation of the Spread of Epidemics with individuals contact using Cellular Automata Modeling, 2012 Fifth International Conference on Information and Computing Science, pp. 60–62.
Zhang, Y., Huang, J., Ding, Y., 2016c. Porous Co3O4/CuO hollow polyhedral nanocages derived from metal-organic frameworks with heterojunctions as efficient photocatalytic water oxidation catalysts. Appl. Catal. B Environ. 198, 447–456.
Zhu, H.-Y., Jiang, R., Xiao, L., 2010. Adsorption of an anionic azo dye by chitosan/kaolin/γ-Fe2O3 composites. Appl. Clay Sci. 48, 522–526.
Zvulunov, Y., Ben-Barak-Zelas, Z., Fishman, A., Radian, A., 2019. A self-regenerating clay-polymer-bacteria composite for formaldehyde removal from water. Chem. Eng. J. 374, 1275–1285.